THE JOURNAL OF BIOLOGICAL CHEMISTRY VOL. 289, NO. 49, pp. 34189–34204, December 5, 2014
Published in the U.S.A.

Nicotinamide Phosphoribosyltransferase Promotes Epithelial-to-Mesenchymal Transition as a Soluble Factor Independent of Its Enzymatic Activity*

Received for publication, July 7, 2014, and in revised form, October 7, 2014 Published, JBC Papers in Press, October 20, 2014, DOI 10.1074/jbc.M114.594721

Debora Soncini[‡1], Irene Caffa[‡1], Gabriele Zoppoli[§¶], Michele Cea[‡‖], Antonia Cagnetta[‖], Mario Passalacqua[‡‡‡], Luca Mastracci[‡‡§§], Silvia Boero[§§], Fabrizio Montecucco[‡¶¶], Giovanna Sociali[**§§§], Denise Lasigliè[‡], Patrizia Damonte[‡], Alessia Grozio[**§§§], Elena Mannino[**§§§], Alessandro Poggi[§§], Vito G. D'Agostino[‖‖], Fiammetta Monacelli[‡], Alessandro Provenzani[‖‖], Patrizio Odetti[‡§§], Alberto Ballestrero[‡§§], Santina Bruzzone[**§§§], and Alessio Nencioni[‡§§2]**

*From the [‡]Department of Internal Medicine, **Department of Experimental Medicine, Section of Biochemistry, and [§§§]Center of Excellence for Biomedical Research, and [‡‡]Department of Integrated Surgical and Diagnostic Sciences, Pathology Unit, University of Genoa, 16132 Genoa, Italy, the [§]Institut Jules Bordet, Université Libre de Bruxelles, 1000 Brussels, Belgium, the [¶]Laboratory of Molecular Pharmacology, Center for Cancer Research, National Cancer Institute, National Institutes of Health, Bethesda, Maryland 20892, the [‖]Jerome Lipper Multiple Myeloma Center, Dana-Farber Cancer Institute, Harvard Medical School, Boston Novartis Institutes for BioMedical Research, Cambridge, Massachusetts 02139, the [§§]Istituto di Ricovero e Cura a Carattere Scientifico Azienda Ospedaliera Universitaria San Martino-Istituto Scientifico Tumori, Istituto Nazionale per la Ricerca sul Cancro, 16132 Genoa, Italy, the [¶¶]Division of Cardiology, Foundation for Medical Researches, Department of Medical Specialties, University of Geneva, 1211 Geneva, Switzerland, the [‖‖]Laboratory of Genomic Screening, Centre for Integrative Biology, University of Trento, 38123 Trento, Italy, and [‡‡‡]Italian Institute of Biostructures and Biosystems, University of Genoa, 16132 Genoa, Italy*

Background: Nicotinamide phosphoribosyltransferase (NAMPT) acts both as an enzyme in the production of the coenzyme NAD^+ and as a secreted cytokine.
Results: In breast cancer cells, NAMPT induces the epithelial-to-mesenchymal transition, a process that underlies metastasis, as a secreted protein independent of its enzymatic activity.
Conclusion: Secreted NAMPT promotes epithelial-to-mesenchymal transition.
Significance: Extracellular NAMPT neutralization may be of therapeutic value.

Boosting NAD^+ biosynthesis with NAD^+ intermediates has been proposed as a strategy for preventing and treating age-associated diseases, including cancer. However, concerns in this area were raised by observations that nicotinamide phosphoribosyltransferase (NAMPT), a key enzyme in mammalian NAD^+ biosynthesis, is frequently up-regulated in human malignancies, including breast cancer, suggesting possible protumorigenic effects for this protein. We addressed this issue by studying NAMPT expression and function in human breast cancer *in vivo* and *in vitro*. Our data indicate that high NAMPT levels are associated with aggressive pathological and molecular features, such as estrogen receptor negativity as well as HER2-enriched and basal-like PAM50 phenotypes. Consistent with these findings, we found that NAMPT overexpression in mammary epithelial cells induced epithelial-to-mesenchymal transition, a morphological and functional switch that confers cancer cells an increased metastatic potential. However, importantly, NAMPT-induced epithelial-to-mesenchymal transition was found to be independent of NAMPT enzymatic activity and of the NAMPT product nicotinamide mononucleotide. Instead, it was mediated by secreted NAMPT through its ability to activate the TGFβ signaling pathway via increased TGFβ1 production. These findings have implications for the design of therapeutic strategies exploiting NAD^+ biosynthesis via NAMPT in aging and cancer and also suggest the potential of anticancer agents designed to specifically neutralize extracellular NAMPT. Notably, because high levels of circulating NAMPT are found in obese and diabetic patients, our data could also explain the increased predisposition to cancer of these subjects.

The aging process is accompanied by a decline in systemic NAD^+ levels, possibly as a result of defective NAD^+ biosynthesis and of poly(ADP-ribose) polymerase-mediated NAD^+ depletion (1). Regardless of the underlying mechanism, declining NAD^+ levels seem to facilitate the occurrence of several age-related diseases, including cancer, because they negatively affect the activity of sirtuins, NAD^+-dependent enzymes with pleiotropic antiaging and tumor-suppressive effects (2). Supplementation of key NAD^+ intermediates, such as nicotinamide, nicotinic acid, nicotinamide mononucleotide (the enzy-

* This work was supported in part by Associazione Italiana per la Ricerca sul Cancro Grant 6108 (to A. N.), by Seventh Framework Project PANACREAS Grant 256986 (to A. N.), by Italian Ministry of Health Project Grant GR-2008-1135635 (to A. N.), by the Compagnia di San Paolo (to A. N.), by the Fondazione Umberto Veronesi (to A. N.), by the University of Genoa, by the PO CRO Fondo Sociale Europeo Regione Liguria 2007–2013 Asse IV "Capitale Umano" (to S. Boero), and by Swiss National Science Foundation Grant 310030_152639/1 (to F. M.).
[1] Both authors contributed equally to this work.
[2] To whom correspondence should be addressed: Dept. of Internal Medicine, University of Genoa, V.le Benedetto XV 6, 16132 Genoa, Italy. Tel.: 39-010-353-8990; Fax: 39-010-353-7989; E-mail: alessio.nencioni@unige.it.

matic product of nicotinamide phosphoribosyltransferase (NAMPT)),[3] and nicotinamide ribose, has been proposed as a promising strategy for preventing and treating various age-associated disorders generated by NAD^+ decline. In this context, it is of interest that both nicotinic acid and nicotinamide showed remarkable anticancer and antimetastatic effects in breast cancer (BC) models (3).

However, controversy has arisen over the exploitation of NAD^+ biosynthesis in cancer because NAMPT, which is one of the key enzymes for NAD^+ production in mammalian cells, has been found to be frequently up-regulated in malignant cells, suggesting that it may exert protumorigenic effects (4). Specifically, strong NAMPT expression was reported in breast, colorectal, brain, stomach, thyroid, endometrial, ovarian, and prostate cancer as well as in multiple myeloma, melanoma, and astrocytomas (4). The possibility that NAMPT could be subjected to regulation by oncogenes has also been proposed recently on the basis of the observation that v-myc avian myelocytomatosis viral oncogene homolog (MYC) promotes NAMPT up-regulation in different cell types (5). Among the mechanisms that have been suggested to explain the role of NAMPT in cancer are the increased metabolic demands of cancer *versus* healthy cells, the ability to stimulate the antiapoptotic effects of SIRT1 (*i.e.* p53 deacetylation), and its propensity to trigger calcium signaling and cell motility (4).

BC is a highly heterogeneous type of cancer that shares many features with other common cancers, including mutations, amplifications, or deletions in key oncogenes and tumor suppressors (*i.e. HER2*, *MYC*, *TP53*, *CDKN2A*, and *PTEN*), an important role of the tumor microenvironment, and the tendency to metastasize through a process named epithelial-to-mesenchymal transition (EMT) (6–8). In addition, similar to other types of cancer, BC is strongly related to age (9) as well as to common lifestyle- and diet-related conditions such as obesity (particularly postmenopausal BC) and diabetes (10, 11). Importantly, although the last two decades have witnessed a remarkable improvement in the prognosis of patients with BC, the death toll of this disease remains high, with 40,000 deaths per year in the United States and over 100,000 deaths in Europe (12, 13). Therefore, further efforts to optimize BC prevention and treatment are required.

Here we addressed the issue of the role of NAMPT in BC by studying its expression in a large data set of primary BC (the METABRIC set) (14) and assessed by which mechanism increased NAMPT levels in mammary epithelial cells could favor tumorigenesis. A new mechanism is described by which, in mammary epithelial cells, NAMPT promotes EMT independent of its enzymatic activity and of its product nicotinamide mononucleotide but, rather, through its function as a cytokine secreted into the extracellular environment.

[3] The abbreviations used are: NAMPT, nicotinamide phosphoribosyltransferase; BC, breast cancer; EMT, epithelial-to-mesenchymal transition; sulforhodamine B; QPCR, quantitative real-time PCR; IHC, immunohistochemistry; eNAMPT, extracellular nicotinamide phosphoribosyltransferase; Glc-6-PD, glucose-6-phosphate dehydrogenase; METABRIC, Molecular Taxonomy of Breast Cancer International Consortium; CCLE, Cancer Cell Line Encyclopedia; PBEF, Pre-B-Cell Colony Enhancing Factor (acronyms: NAMPT, visfatin); MANOVA, multivariate analysis of variance or multiple analysis of variance; CGH, comparative genomic hybridization; ER, estrogen receptor; PGR, progesterone receptor; PAM, prediction analysis of microarray.

EXPERIMENTAL PROCEDURES

Cell Lines and Reagents—MCF10A, MCF7, T47D, MDA-MB-231, BT549, MDA-MB-468, and Phoenix cells were purchased from the ATCC. HMLE cells were a gift from Dr. Robert A. Weinberg (Whitehead Institute for Biomedical Research, Cambridge, MA). MCF10A and HMLE cells were cultured in MCF10A medium (DMEM/F12 (Invitrogen) supplemented with 5% horse serum, antibiotics, insulin (0.01 mg/ml), hydrocortisone (500 ng/ml), EGF (20 ng/ml), and cholera toxin (100 ng/ml) (all from Sigma-Aldrich, Milan, Italy)). Phoenix, MCF7, T47D, MDA-MB-231, BT549, and MDA-MB-468 cells were maintained in RPMI 1640 medium supplemented with 10% FBS (Invitrogen) and antibiotics. Puromycin, nicotinamide, and protease/phosphatase inhibitor mixture were purchased from Sigma-Aldrich. FK866 was provided by the National Institute of Mental Health Chemical Synthesis and Drug Supply Program, and CHS 828 was purchased from Cayman Chemical. AZD5363 and GDC-0068 were from Selleck Chemicals, and LY294002 and SB431542 were from Sigma-Aldrich. Recombinant human NAMPT (produced in HEK 293 cells) was from Adipogen (San Diego, CA).

Doubling Time Measurement and Cell Growth Assays—For cell doubling time estimation, 10^5 cells/well were plated in 6-well plates and allowed to adhere overnight. At 0, 12, 36, and 48 h, cells were fixed with 3% TCA for 1 h at 4 °C. Thereafter, plates were air-dried, stained for 1 h with 0.4% sulforhodamine B (SRB) in 1% glacial acetic acid, rinsed three times with 1% glacial acetic acid, and air-dried again. SRB was dissolved in 10 mM Tris, and optical density was measured at 515 nm on a Tecan Infinte F200 Pro plate reader. Doubling time was finally calculated from the signal corresponding to the different time points. For cell growth assays, $1–5 \times 10^3$ cells/well were plated in 96-well plates and allowed to adhere overnight. Thereafter, cells were either fixed with 3% TCA or stimulated with or without FK866 (10, 100, and 1000 nM). 72 h later, cells were fixed with 3% TCA and stained with SRB, and cell growth was calculated as detailed in Ref. 15.

Plasmids—pQCXIP-IRES-PURO (pQXCIP) and pQCXIP-NAMPT-IRES-PURO were a gift from Dr. J. Geoffrey Pickering (Robarts Research Institute, University of Western Ontario, London, ON, Canada) (16). pQXCIP-NAMPT H247A was generated by site-specific mutagenesis utilizing the QuikChange XL kit (Stratagene, catalog no. 200516) according to the instructions of the manufacturer.

Retroviral Transduction—For retroviral transductions, 10^6 Phoenix cells were plated in 4 ml medium in 6-cm dishes and allowed to adhere for 24 h. Thereafter, cells were transfected with 4 μg of plasmid DNA using TransIT-293 (Mirus Bio, Madison, WI) according to the instructions of the manufacturer. Viral supernatants were harvested after 36, 48, 60, and 72 h and used to infect MCF-10A cells (3×10^5) in 10-cm dishes in the presence of 5 μg/ml protamine sulfate. Successfully infected cells were selected using 1.3 μg/ml puromycin.

NAMPT Silencing by RNAi—NAMPT silencing in MDA-MB-231 was performed using pLKO.1 plasmids as described previously (17). The sequences of the NAMPT silencing sequences were as follows: shRNA#1, 5′-GTAACTTAGATG-GTCTGGAAT-3′; shRNA#2, 5′-GAAGCCAAAGATGTC-TACAAA-3′. As a control, a pLKO.1 plasmid encoding for a scrambled shRNA was purchased from Addgene (Cambridge, MA, plasmid no. 1864). In brief, pLKO.1 plasmids were cotransfected with the packaging plasmids pVSV-G and δ8.9 into 293T cells with Transit293 (Mirus Bio). 48 and 72 h after transfection, the supernatants were harvested, filtered, and used to infect MDA-MB-231 (which had been plated the day before in 6-cm dishes at 3×10^5 cells/dish) in the presence of 5 μg/ml protamine sulfate. Successfully infected cells were subsequently selected with 1.2 μg/ml puromycin.

Immunoblotting—Unless otherwise specified, 3×10^5 cells were plated in 6-well plates and allowed to adhere for 24 h. Thereafter, cells were lysed in lysis buffer (50 mM Tris-HCl (pH 7.5), 150 mM NaCl, 1% Nonidet P-40, and protease inhibitor mixture), and protein concentration was determined according to a standard Bradford assay. Proteins (30 μg) were separated by SDS-PAGE, transferred to a PVDF membrane (Immobilon-P, Millipore, Vimodrone, Italy), and detected with the following antibodies: anti-NAMPT (anti-PBEF, catalog no. A300-372A, Bethyl Laboratories, Inc., Montgomery, TX), anti-E-cadherin (catalog no. 3195, Cell Signaling Technology, Danvers, MA), anti-vimentin (catalog no. 5741, Cell Signaling Technology), anti-Claudin1 (catalog no. 4933, Cell Signaling Technology), anti-ZO1 (catalog no. 8193, Cell Signaling Technology), anti-phospho-AKT (Ser-473, catalog no. 9271, Cell Signaling Technology), anti-AKT (catalog no. 9272, Cell Signaling Technology), anti-phospho-ERK p42/p44 (Thr-202/Tyr-204, catalog no. 4377, Cell Signaling Technology), anti-ERK (catalog no. 9102, Cell Signaling Technology), phospho-SMAD3 (Ser-423/425, catalog no. sc-11769, Santa Cruz Biotechnology), SMAD3 (catalog no. sc8332, Santa Cruz Biotechnology), and anti β-actin-HRP (catalog no. sc-47778, Santa Cruz Biotechnology) using standard ECL. Band intensities were quantified with the ChemiDoc imaging system (Bio-Rad).

Immunostaining and Flow Cytometry—3×10^5 cells were plated in 6-well plates and allowed to adhere for 24 h. Subsequently, cells were detached, washed, and stained for 30 min at 4 °C with a CD24-PerCP-Cy5.5 antibody (catalog no. 561647) and a FITC-anti-CD44 antibody (catalog no. 555478), both from BD Biosciences. Cells were analyzed on a FACSCalibur by acquiring 10,000 events.

Determination of Intracellular NAD^+ Levels—For intracellular NAD^+ quantification, 10^5 cells/well were incubated in 6-well plates for 48 h in the presence or absence of FK866 (300 nM). Thereafter, cells were harvested and lysed in 0.1 ml 0.6 M perchloric acid at 4 °C. Intracellular NAD^+ levels were determined as in Ref. 18.

Glucose-6-Phosphate Dehydrogenase Activity Assay—10^5 cells/well were plated in 6-well plates in 1 ml of culture medium. Supernatants were collected 48 h later and used for glucose-6-phosphate dehydrogenase (Glc-6-PD) activity assays. In brief, media were centrifuged to remove intact cells. 50 μl of supernatant from each cell type was added to 950 μl of the assay mixture (0.1 M Tris-HCl (pH 8), 0.5 mM EDTA, 10 mM $MgCl_2$, 0.2 mM $NADP^+$, and 0.6 mM glucose-6-P), and absorbance at 340 nm was spectrophotometrically detected for 5 min to determine Glc-6-PD activity. Intracellular Glc-6-PD activity was measured on cell lysates (40 μg of proteins was added to the assay mixture).

ELISA for NAMPT and TGFβ1 Detection in Cell Supernatant—Cellular supernatants were assayed for eNAMPT and TGFβ1 concentration using commercially available NAMPT and TGFβ1 ELISA kits (Adipogen SA and R&D Systems, respectively). In the case of supernatants generated from cell lines with different proliferation rates, to allow comparisons, ELISA results were normalized to cell densities at the time of supernatant harvest as detected by SRB staining (see above).

eNAMPT Immunodepletion from Cell Supernatants—10^6 cells were plated in 75 cm^2 cell culture flasks. Supernatants were harvested when cells reached 70–80% confluence, spun at $1200 \times g$ at 4 °C for 5 min to remove intact cells and stored at 4 °C until subsequent use. 500 μl of Dynabeads protein G for immunoprecipitation (Invitrogen) was washed twice with PBS-Tween (Tween 0.02%) with the aid of a magnetic 15-ml tube holder (M-Medical). Subsequently, the beads were resuspended in 250 μl of PBS and incubated on a tube rotator for 30 min at room temperature after the addition of 80 μl of anti-NAMPT antibody (anti-PBEF, catalog no. A300-372A, Bethyl Laboratories, Inc.). Thereafter, the beads were washed twice with PBS and incubated overnight with 10 ml of cell supernatants on a tube rotator at 4 °C. Finally, the beads were removed from the supernatants using a magnetic tube holder. Supernatants were sterile-filtered and stored at 4 °C until subsequent use.

Quantitative Real-time PCR (QPCR)—Total RNA was extracted from cells using the RNeasy mini kit (Qiagen, Milan, Italy) according to the instructions of the manufacturer. 1 μg of RNA was reverse-transcribed in a final volume of 50 μl using a high-capacity cDNA reverse transcription kit (Invitrogen). 5 μl of the resulting cDNA was used for QPCR with a 7900 HT fast real-time PCR instrument (Applied Biosystems by Invitrogen). NAMPT (forward, 5′- AGCCGAGTTCAACATCCTCCT-3′; reverse, 5′-AGACATCTTTGGCTTCCTGGAT-3′), E-cadherin (forward, 5′-TGCCCAGAAAATGAAAAAGG-3′; reverse, 5′-GTGTAT-GTGGCAATGCGTTC-3′), N-cadherin (forward, 5′-ACAGTG-GCCACCTACAAAGG-3′; reverse, 5′-CCGAGATGGGGTT-GATAATG-3′), vimentin (forward, 5′-GAGAACTTTGC-CGTTGAAGC-3′; reverse: 5′-GCTTCCTGTAGGTGGCA-ATC-3′), fibronectin (forward, 5′-CAGTGGGAGACCTCGAG-AAG-3′; reverse, 5′-TCCCTCGGAACATCAGAAAC-3′), and ZEB1 (forward, 5′-GAAAATGAGCAAAACCATGATCCTA-3′; reverse, 5′-CAGGTGCCTCAGGAAAAATGA-3′), mRNA levels were detected using SYBR Green GoTaq® QPCR Master Mix (Promega, Milan, Italy) according to the protocol of the manufacturer. Gene expression was normalized to housekeeping gene expression (β-actin). Comparisons in gene expression were calculated using the $2^{-\Delta\Delta Ct}$ method.

Light Microscopy—Cells were imaged at room temperature using the ×10 magnification of a Zeiss AXIOVERT200 microscope and an Olympus C-4040ZOOM camera. The image files

were acquired with Olympus CAMEDIA Master 2.5 software and subsequently processed using Microsoft Photo Editor.

Confocal Microscopy—3×10^4 MCF10A vector or NAMPT cells were plated on glass coverslips (Thermo Scientific Nunc Lab-Tek II chamber slide system) and allowed to adhere overnight. Cells were then fixed with 4% paraformaldehyde, washed, saturated, and incubated with anti E-cadherin or anti-vimentin primary antibody overnight at 4 °C. Specific staining was visualized with a goat anti-rabbit Alexa Fluor 488 secondary antibody (Molecular Probes, Eugene, OR), and nuclei were counterstained with Qnuclear™ deep red stain (Invitrogen). Then glass coverslip were mounted using Prolong Gold antifade reagent (Invitrogen). The images were collected using a three-channel TCS SP2 laser-scanning confocal microscope (Leica Microsystems, Wetzlar, Germany).

Statistical Analysis—Each experiment was repeated at least three times. Statistical analyses were performed with GraphPad Prism software version 5 (GraphPad Software) using one-way analysis of variance for multiple group comparisons or unpaired Student's *t* test for two-group comparisons. *p* values below 0.05 were considered significant. For the statistical analyses of data from the METABRIC (14) and the Cancer Cell Line Encyclopedia (19) data sets, correlations of gene transcripts were performed using Pearson's correlations, with Holm's adjusted *p* values of less than 0.01 considered significant. Comparison of *NAMPT* levels in ER-positive *versus* ER-negative tumors was done using Welch two-sample *t* test ($\alpha = 0.01$). One-way analysis of variance models, with Tukey contrast multiple comparisons of means and single-step adjusted *p* values (adjusted $\alpha = 0.05$) were used to assess differences in *NAMPT* expression for tumor features with more than two categorical levels. A MANOVA model including all of the statistically significant variables at univariate analysis and their interactions, entered in a backward/forward stepwise fashion, was used for multivariate assessment of potential associations between the aforementioned BC characteristics and *NAMPT* expression. Variables with an adjusted $\alpha < 0.05$ were reported as significant. All analyses were two-sized. Statistical calculations and related plots were performed using R v. 3.01 and the packages Rcmdr, stats, survival, and car.

NAMPT Detection in Primary Tumor Specimens by Immunohistochemistry (IHC)—NAMPT expression was evaluated in a cohort of 40 patients treated at our center between 2008 and 2011. This study was approved by the Ethics Committee of the IRCCS AOU San Martino-IST, Genoa, Italy (Protocol 01/2013). For each selected paraffin block, two 4-μm serial sections were cut. One section was stained with H&E, and the other was mounted on SuperFrost Plus slides and made available for IHC. IHC for NAMPT was performed using the anti-NAMPT rabbit polyclonal antibody H-300 (Santa Cruz Biotechnology) as described in Lee *et al.* (20). Slides were imaged using ×20 magnification of an Olympus BX61 microscope. NAMPT expression scoring was done according to Lee *et al.* (20). Tumors were staged according to the TNM classification of malignant tumors (TNM). Human epidermal growth factor receptor 2 (HER2), estrogen receptor (ER), and progesterone receptor (PGR) expression were evaluated by routine diagnostic IHC.

RESULTS

NAMPT Expression in BC Is Associated with Estrogen Receptor-negative, HER2-enriched, and Basal-like Tumors—We assessed *NAMPT* mRNA expression in the METABRIC discovery set (14), a clinically annotated, publicly available BC gene expression microarray data set. This data collection contains complete information from 517 patients with tumor stages 1–4, including tumor size, histological grading, staging, hormone receptor status, *HER2* amplification status as assessed by array-CGH, and intrinsic phenotype according to the PAM50 classification (21). The METABRIC data set also presents the unique advantage of coming together with a validation set of similar size for the confirmation of statistical associations. In the aforementioned discovery set, *NAMPT* showed a wide expression range, with a more than 4-fold log2 change between the lowest and the highest expresser tumors (mean 6.8, range 5.4–9.5, S.D. 0.6). Given the high variability of *NAMPT* expression in BC, we searched for biological and clinical features that would account for such an observation. We observed that ER status, histological grading, and the PAM intrinsic phenotype classification were associated with different *NAMPT* levels at univariate analysis (Fig. 1, *A–C*) whereas stage, primary tumor size, age, menopausal status, and *HER2* amplification status as determined by array-CGH were not. In particular, *NAMPT* levels were higher in ER-negative *versus* ER-positive tumors ($p = 1.7 \times 10^{-5}$, Fig. 1*A*), in higher *versus* lower grade cancers (F test $p = 0.0009$, Tukey contrast multiple comparison test for high *versus* low and high *versus* intermediate grade adjusted single-step $p < 0.05$, Fig. 1*B*), and in HER2-enriched, basal-like, and normal-like tumors *versus* luminal A and B tumors (F test $p = 1.8 \times 10^{-10}$, Tukey contrast multiple comparison test for the aforementioned comparisons adjusted single-step $p < 0.05$ or less, Fig. 1*C*). ER status and PAM50 intrinsic phenotype remained statistically significant in the validation dataset ($n = 531$), where the pairwise comparison for PAM50 remained significant for basal-like *versus* luminal A and B tumors with an adjusted *p* value of less than 0.001, as well as between HER2-enriched tumors and luminal ones ($p < 0.05$). Histological grade showed a non-significant trend in the same direction of the analysis performed in the training set.

A multivariate one-way analysis of variance model including all of the statistically significant variables of the univariate analysis and their interactions was also utilized. Here only the PAM50 intrinsic phenotype classification was initially found to be independently associated with *NAMPT* levels ($p = 0.0003$). However, in the validation set, the associations between *NAMPT* expression, on the one hand, PAM50 ($p = 0.0096$), ER status ($p = 0.003$), and their interaction ($p = 0.02$), on the other, were all found to be significant.

In conclusion, high *NAMPT* levels are associated with negative hormonal receptor status as well as with the basal-like and the HER2-enriched PAM intrinsic phenotypes in BC. The overall significance of the association between these biological features and *NAMPT* levels appears to be high, although other, still unknown factors must clearly contribute to determine *NAMPT* expression, as evidenced by the moderate size effect of the model in the discovery set. It is presently unclear how to inter-

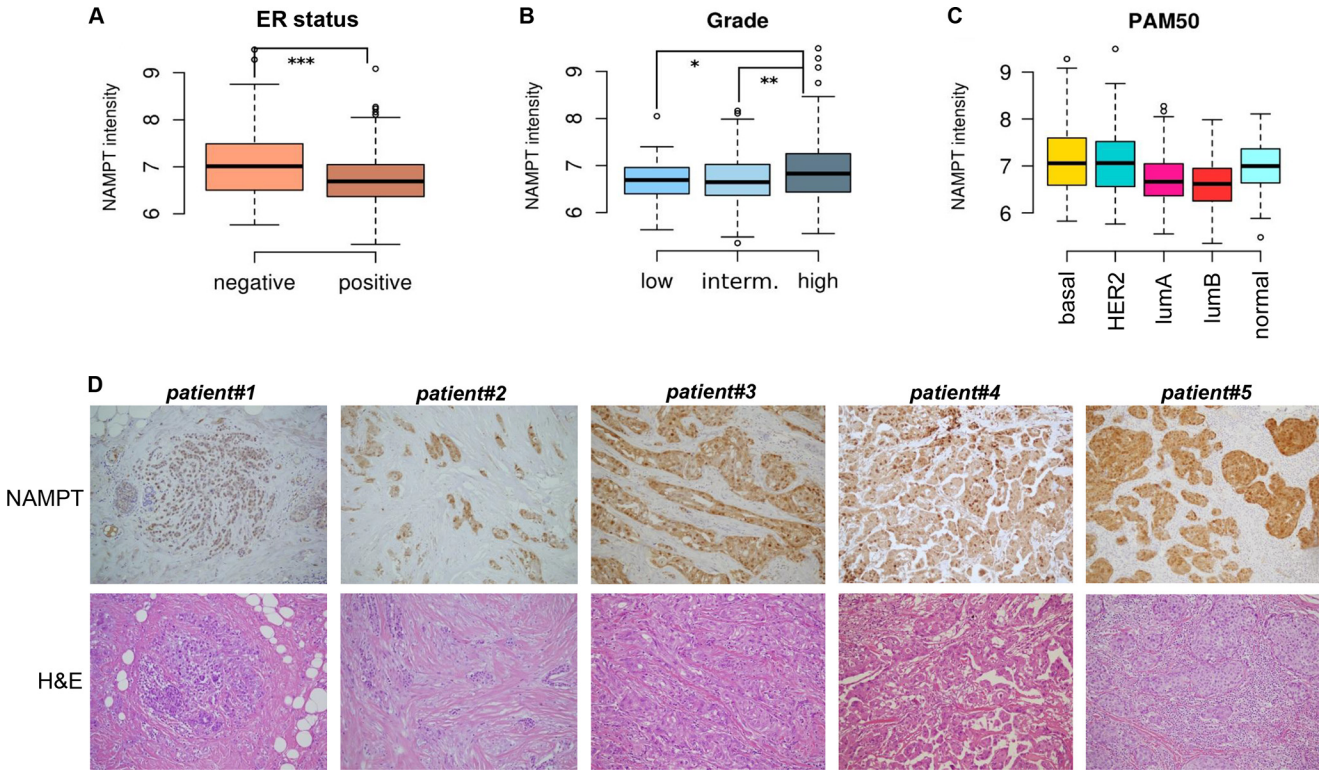

FIGURE 1. **NAMPT expression is associated with ER-negative, basal-like, and HER2-enriched BC.** *A*, *NAMPT* expression stratified by ER status. *y axis*, normalized log2 intensity; *thick horizontal lines*, means; *boxes*, 25–75th percentiles; *whiskers*, 95% percentiles; *open circles*, outliers. *B*, *NAMPT* expression stratified by histological grade. *interm*, intermediate. *C*, *NAMPT* expression stratified by the intrinsic phenotype classification (PAM50). *HER2*, HER2-enriched; *normal*, normal-like. *A* and *B*, brackets represent statistically significant pairwise comparisons. *, $p < 0.05$; **, $p < 0.01$; ***, $p < 0.001$. For graphical limitations, brackets in *C* are not reported. *D*, NAMPT expression as detected by IHC and H&E staining in five primary BCs. Patient and tumor features were as follows. Patient#1: age at diagnosis, 51; histology, lobular breast cancer; stage, pT1c; ER 95%; PGR 90%; NAMPT score, 3. Patient#2: age at diagnosis, 39; histology, ductal breast cancer; stage, pT2; ER 90%; PGR 90%; NAMPT score, 4. Patient#3: age at diagnosis, 59; histology, ductal breast cancer; stage, pT1c; ER negative; PGR negative; NAMPT score, 4. Patient#4: age at diagnosis, 49; histology, apocrine breast cancer; stage, pT2; ER negative; PGR negative; NAMPT score, 3. Patient#5, age at diagnosis, 46; histology, ductal breast cancer; stage, pT1c; ER 95%; PGR 80%; NAMPT score, 4.

pret the results for the normal-like phenotype, especially in light of the criticism pointing toward a possible bias for this cluster as actually including tumors from other phenotypes but with an overall low cellularity that precludes a precise classification (22).

Using IHC, Lee *et al.* (20) found previously that NAMPT expression in BC was predominantly confined to the malignant cells rather than to the adjacent non-cancerous tissues . Similar patterns of NAMPT expression we observed in a cohort of patients treated at our center ($n = 40$), of which five representative cases are presented in Fig. 1*D*. These findings suggest that the aggressive biological features of BCs expressing high *NAMPT* are probably mediated by the NAMPT produced by tumor cells. Nevertheless, because *NAMPT* is also expressed by white blood cells, some of which (such as macrophages) have been ascribed a role in mammary carcinogenesis (23), we also searched for possible correlations between *NAMPT* and leukocyte markers in the METABRIC data set. Specifically, *STAT1* and *CD45* (*PTPRC*) were used as proxies for tumor-infiltrating leukocytes (24). Although no statistical association between *NAMPT* and *STAT1* was found ($p = -0.074$), a correlation between *NAMPT* and *CD45* expression could be detected ($p = 0.42$), raising the theoretical possibility that infiltration by protumorigenic leukocytes may be responsible for the increased aggressiveness of BCs expressing high *NAMPT* (23). Therefore, we aimed to assess whether *NAMPT* overexpression in mammary epithelial cells would be sufficient to confer on them adverse biological features and to elucidate the underlying mechanism(s).

NAMPT Promotes EMT in Mammary Epithelial Cells—NAMPT was overexpressed in the non-tumorigenic breast epithelial cell line MCF10A by retroviral transduction (Fig. 2*A*). Morphological examination of these cells readily revealed the acquisition of an elongated fibroblast-like phenotype (Fig. 2*B*), suggesting that NAMPT overexpression could have caused an EMT (7, 25). EMT is a complex change in cell function upon which epithelial cells switch from a polarized, epithelial phenotype to a mesenchymal status, which makes them prone to leave the epithelial layer where they belong and migrate to distant sites (7, 25). Hallmarks of EMT in BC cells include *E-cadherin* down-regulation and the expression of mesenchymal genes such as *N-cadherin*, *vimentin*, and *fibronectin* (26). In mammary epithelial cells, EMT is also typically accompanied by the acquisition of a $CD24^{low}/CD44^{high}$ phenotype (27). In line with the hypothesis that NAMPT-overexpressing MCF10A cells (NAMPT-MCF10A) had undergone EMT, they were found to exhibit markedly reduced *E-cadherin* levels compared with control cells by QPCR, whereas *N-cadherin*, *vimentin*, and *fibronectin* mRNAs were all up-regulated (Fig. 2*C*). NAMPT overexpression was associated with a markedly reduced expres-

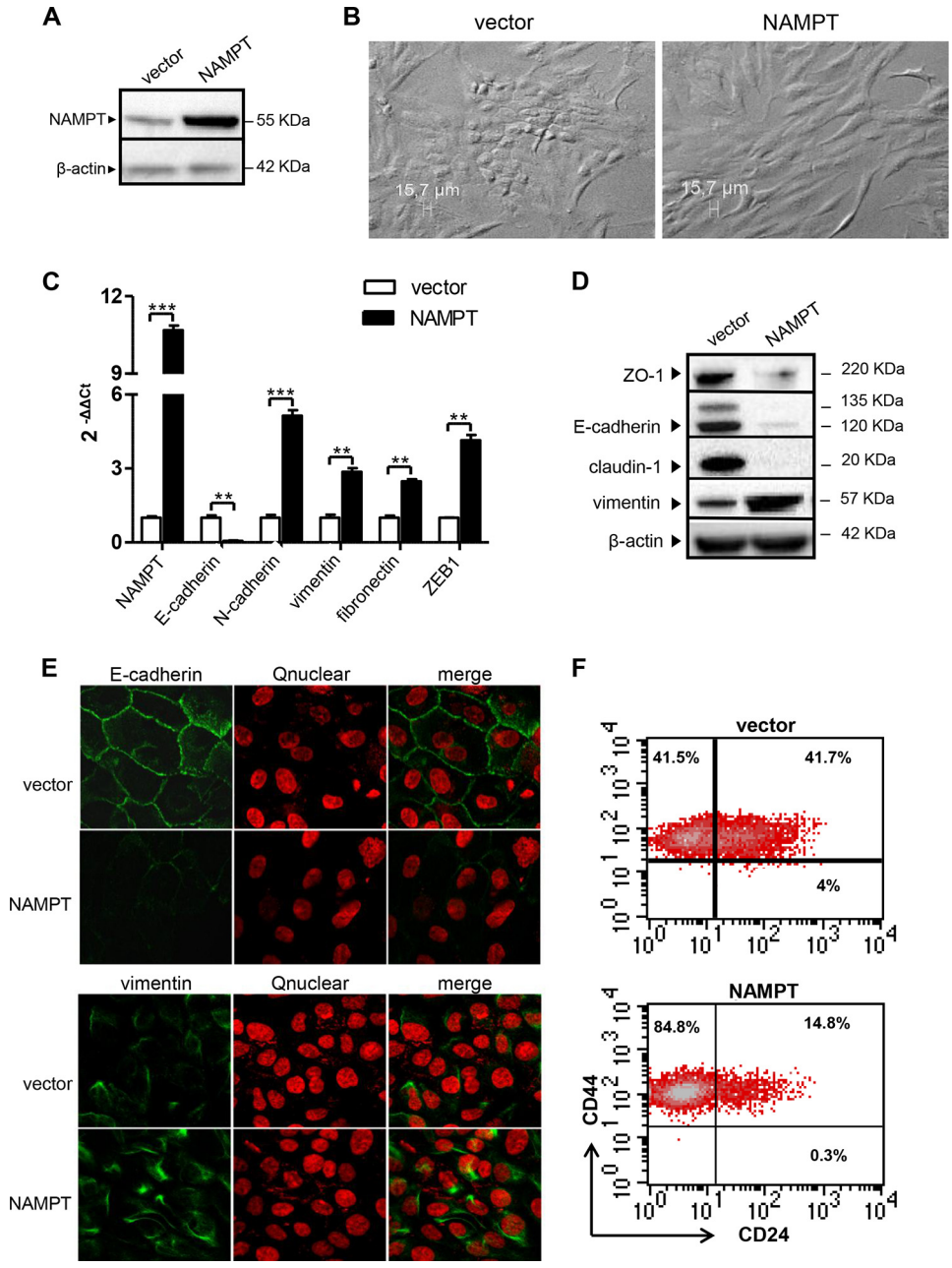

FIGURE 2. **NAMPT overexpression induces EMT-like cellular changes in MCF10A cells.** *A–F*, MCF10A cells were transduced with human NAMPT or with a control vector (*vector*). Thereafter, cells were imaged by light microscopy or used for RNA isolation, protein lysate generation, confocal microscopy, or flow cytometry analyses. One representative experiment of three is presented. *A*, NAMPT and β-actin levels in protein lysates were detected by immunoblotting. *B*, the fibroblast-like morphology of NAMPT-MCF10A in a representative light microscopy image. *C*, *NAMPT*, *E-cadherin*, *N-cadherin*, *vimentin*, *fibronectin*, and *ZEB1* mRNA levels in NAMPT-MCF10A and vector cells were quantified by QPCR. **, $p < 0.01$; ***, $p < 0.001$. *D*, ZO-1, claudin, vimentin, E-cadherin, and β-actin levels were detected by immunoblotting. *E*, E-cadherin and vimentin representation and distribution in NAMPT-MCF10A and vector cells were assessed by confocal microscopy. *F*, CD24 and CD44 expression on NAMPT-MCF10A and vector cells was evaluated by flow cytometry.

sion of the tight junction proteins ZO-1 and Claudin-1, as detected by Western blotting, whereas the same type of analysis confirmed the strong down-regulation in E-cadherin and the up-regulation of vimentin (Fig. 2*D*). Confocal microscopy readily showed the loss of E-cadherin expression at the cell membrane level in NAMPT-MCF10A, whereas intracellular vimentin expression was increased in the same cells (Fig. 2*E*). Finally, flow cytometry analysis of NAMPT-MCF10A and control cells showed that the former had down-regulated CD24 expression and had switched to a $CD24^{neg}/CD44^{high}$ phenotype (Fig. 2*F*) (6, 14). Therefore, these findings are consistent with high NAMPT expression promoting EMT in MCF10A cells. Notably, compared with the control cells, NAMPT-MCF10A also exhibited a 4-fold increase in the mRNA levels of ZEB1 (Fig. 1*C*), a zinc finger transcription factor that acts as a transcriptional repressor of *E-cadherin* and that has been associated previously with the occurrence of EMT (25).

In MCF10A, cadherin switching has been reported to be influenced by cell confluence, with sparse cultures favoring N-cadherin over E-cadherin expression and, *vice versa*, conflu-

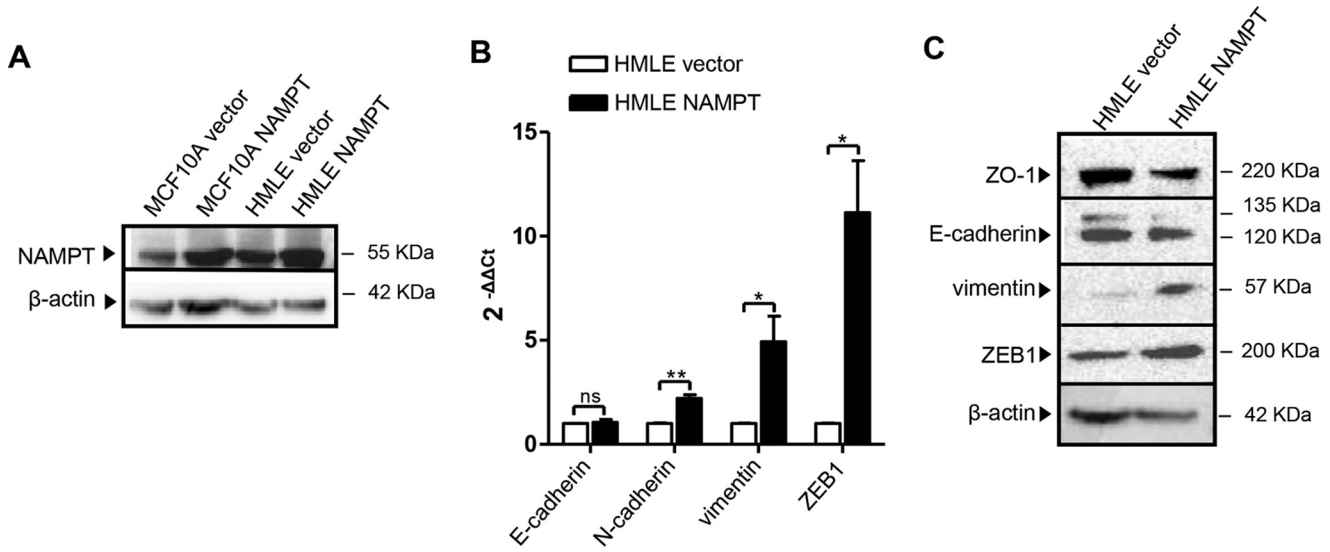

FIGURE 3. **NAMPT overexpression induces the expression of mesenchymal markers in HMLE mammary epithelial cells.** HMLE and MCF10A cells were transduced with human NAMPT or with a control vector (*vector*). Thereafter, cells were used for RNA isolation or for protein lysate generation. *A*, NAMPT and β-actin levels in NAMPT-MCF10A, NAMPT-HMLE, and in the respective vector control cells were detected by immunoblotting. *B*, *NAMPT*, *E-cadherin*, *N-cadherin*, *vimentin*, and *ZEB1* mRNA levels in NAMPT-HMLE and vector cells were quantified by QPCR. *, $p < 0.05$; **, $p < 0.01$; *ns*, not significant. *C*, ZO-1, E-cadherin, vimentin, ZEB1, and β-actin levels in NAMPT-HMLE cells and in their vector cells were detected by immunoblotting. *A–C*, one representative experiment of three is presented.

ent cultures favoring E-cadherin expression and tight junction formation (28). In our experiments, vector MCF10A and NAMPT-MCF10A were found to have comparable doubling times (29.15 and 29.98 h, respectively), were always plated in equal numbers, and their cultures were always closely monitored to avoid that obvious differences in cell confluence may skew the results of our analyses. Therefore, the reported differences between NAMPT-MCF10A and control cells in terms of epithelial and mesenchymal markers are extremely unlikely to reflect differences in cell confluence between the two cell lines.

To assess whether the findings in MCF10A could be reproduced in a different cellular model, NAMPT was also overexpressed by retroviral transduction in HMLE cells (another nontumorigenic breast epithelial cell line (27)). In this second cell line, which we found to have higher baseline NAMPT levels compared with MCF10A (1.5- to 2-fold, Fig. 3*A*), NAMPT overexpression also resulted in *vimentin*, *N-cadherin*, and *ZEB1* up-regulation even though *E-cadherin* was not affected (Fig. 3*B*). Western blot analyses confirmed that NAMPT-HMLE expressed higher vimentin and ZEB1 levels but similar E-cadherin amounts compared with the control cells (Fig. 3*C*). In addition, ZO-1 down-regulation in NAMPT-HMLE was also documented. Overall, these findings indicate that HMLE cells also up-regulate mesenchymal markers and ZEB1 in response to NAMPT overexpression, although the persistence of E-cadherin suggested that, in this cell line, NAMPT-induced EMT was possibly not as complete as the one observed in MCF10A.

NAMPT Is Highly Expressed in Mesenchymal-like BC Cell Lines—We subsequently reasoned that, if high NAMPT promotes EMT, mesenchymal-like BC cell lines should express higher NAMPT levels compared with luminal lines (29). Indeed, in full agreement with this hypothesis, within the cell line panel tested, the three mesenchymal-like BC cell lines MDA-MB-231, BT549, and MDA-MB-468 were expressing the highest amounts of NAMPT, whereas NAMPT levels in luminal MCF7 and T47D cells were the lowest (comparable with those observed in plain MCF10A) (Fig. 4, *A* and *B*). Because NAMPT is also secreted by cells (extracellular NAMPT (eNAMPT)) and acts as an adipocytokine in the extracellular environment (4), we also monitored eNAMPT levels in the supernatants of these cell lines using a commercially available ELISA. Once again, MDA-MB-231, BT549, and MDA-MB-468 cells produced the highest eNAMPT amounts, whereas eNAMPT concentrations in media from MCF7 and T47D cells were the lowest in the entire panel (Fig. 4*C*). Additional data supporting a correlation between NAMPT and mesenchymal features of BC cells came from the statistical analysis of data from the Cancer Cell Line Encyclopedia (CCLE), a publicly available data set of DNA copy number, mRNA expression, and mutation data from 1000 cancer cell lines, including 60 BC cell lines (19). Specifically, within the CCLE BC cell line panel, we found a strong correlation between the expression of *NAMPT* on the one hand and that of *vimentin*, *fibronectin* (Fig. 4, *D* and *E*), *SNAI1* ($p = 0.52$), and *SNAI2* ($p = 0.59$) (SNAI1/2 being transcription factors with a key role in EMT (25)) on the other. Finally, it is noteworthy that a remarkable association between *NAMPT* and *vimentin* in the clinical METABRIC data set was also present (Fig. 4*F*). Therefore, these analyses indicated a strong link between NAMPT and mesenchymal features in BC cell lines and in primary tumors, further supporting the notion that NAMPT promotes EMT.

EMT Induction by NAMPT Is Independent of its Enzymatic Activity—NAMPT is a key enzyme for NAD^+ biosynthesis in mammalian cells, allowing the reconversion of nicotinamide (the main degradation product of NAD^+ itself) back to NAD^+ (1, 30). Specifically, NAMPT catalyzes the condensation of nicotinamide with 5-phosphoribosyl-1-pyrophosphate to yield nicotinamide mononucleotide (31). The latter is subsequently converted to NAD^+ by nicotinamide mononucleotide adenilyltransferases (NMNAT1–3) (31). We conducted several exper-

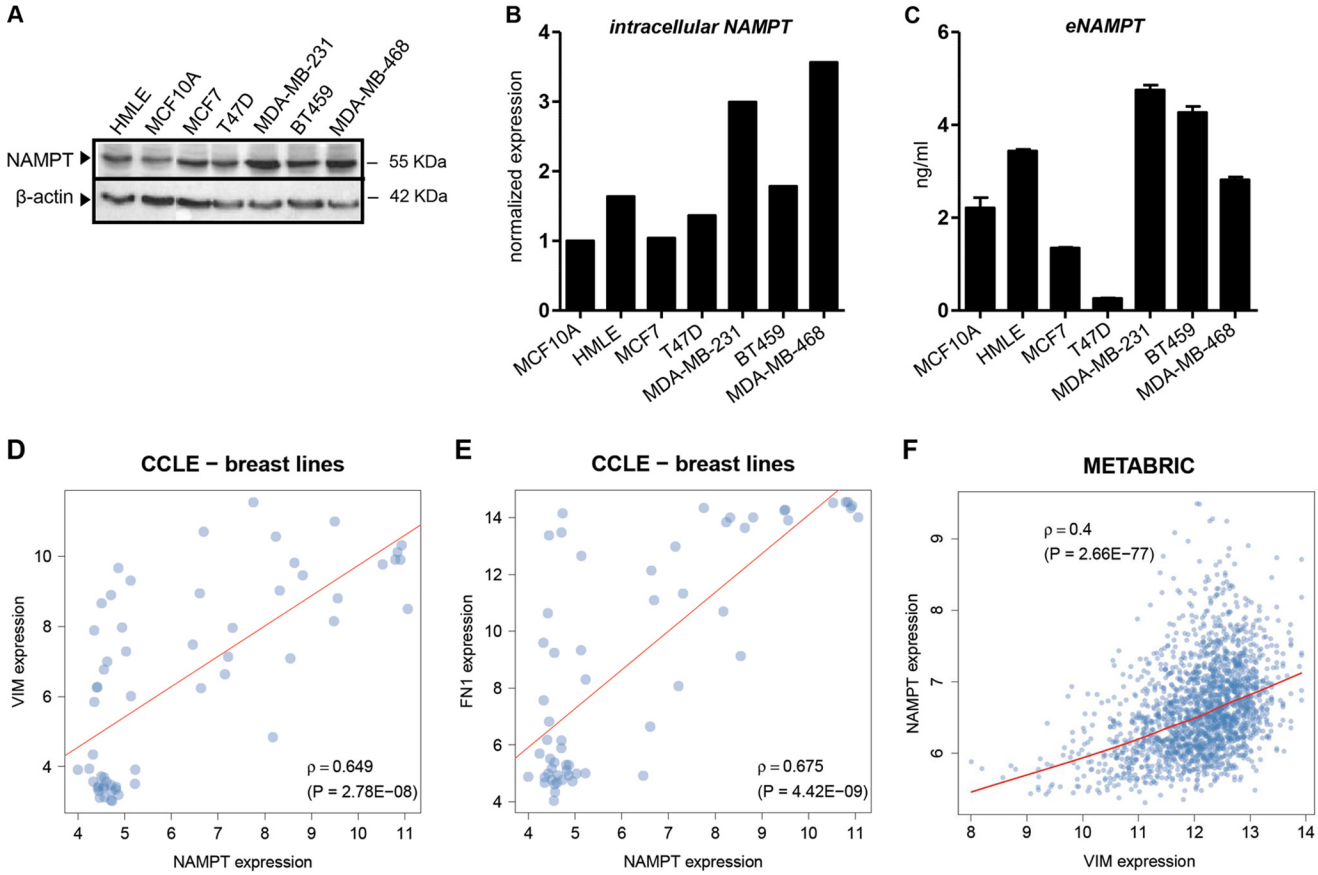

FIGURE 4. **NAMPT is highly expressed in mesenchymal-like BC cell lines, and its expression is associated with mesenchymal markers in CCLE BC cell lines and in the METABRIC data set.** *A–C*, 1–3 × 10^5 MCF10A, HMLE, MCF7, T47D, MDA-MB-231, BT549, or MDA-MB-486 cells/well were cultured in 2 ml of medium in 6-well plates for 48 h. Thereafter, supernatants were harvested, and cells were either used for protein lysate preparation or fixed with TCA, stained with sulforhodamine B, and utilized for ELISA result normalization. One representative experiment of three is presented. *A* and *B*, NAMPT and β-actin levels were detected by immunoblotting. Band intensities were quantified, and, after normalization to β-actin, NAMPT expression in each cell line was compared with its levels in MCF10A cells. *C*, eNAMPT levels in cell supernatants were quantified by ELISA. Results were normalized to cell density as measured by SRB. *D* and *E*, scatter plot representations of *NAMPT versus vimentin* (*VIM*) and *fibronectin* (*FN1*) expression in CCLE BC cell lines. *F*, scatter plot representations of *NAMPT versus* vimentin expression in the METABRIC dataset.

iments to ascertain whether NAMPT-induced EMT would be dependent on NAMPT enzymatic activity. In the first place, we assessed NAD^+ levels in NAMPT-MCF10A *versus* vector cells and found that NAMPT overexpression did not increase intracellular NAD^+ (Fig. 5*A*). Thereafter, we attempted to revert EMT in NAMPT-MCF10A cells by treating them with FK866, a well characterized NAMPT inhibitor (IC_{50} = 0.14 nM) (32). Incubation with 300 nM FK866 (a concentration that largely exceeded its IC_{50} and that has been found previously to be sufficient to induce biological effects in FK866-sensitive cellular models (18)) blunted intracellular NAD^+ concentration by ~25% in NAMPT-MCF10A (Fig. 5*A*) but not in control MCF10A cells, although a trend toward a reduction could be observed in these cells, too. Despite its ability to lower intracellular NAD^+ in NAMPT-MCF10A, FK866 failed to revert *E-cadherin* down-regulation, as well as *N-cadherin*, *vimentin* and *ZEB1* up-regulation, in these cells even after a 2-week incubation (Fig. 5*B*). Similar results were obtained with CHS 828, an unrelated NAMPT inhibitor (IC_{50} = 0.07 nM) (Fig. 5*B*) (33). Notably, FK866 failed to restore *E-cadherin* expression in NAMPT-MCF10A even when added to the cell culture medium from the moment of MCF10A cell transduction with NAMPT (data not shown), therefore making it unlikely that NAMPT enzymatic activity could confer an early imprinting to MCF10A cells (in terms of EMT induction) that cannot be subsequently reverted. It is also noteworthy that, different from other cell types, MCF10A cells were found to be extremely resistant to the cytotoxic activity of the NAMPT inhibitors tested. This feature, which has been noted previously by Cerna *et al.* (34) and which is shared by HMLE cells, too, could be explained by the fact that barely any reduction in NAD^+ levels in response to FK866 could be detected in these cells, whereas other cell types, such as T-lymphocytes, undergo a much more pronounced NAD^+ depletion and eventually die in response to a protracted incubation with these compounds (18). Attempts were also made to recreate the effects of NAMPT overexpression in MCF10A cells by supplementing the cell culture medium with nicotinamide mononucleotide, the product of NAMPT catalytic activity, or with other NAD^+ precursors whose addition into cell culture we found previously to result in increased intracellular NAD^+ concentrations, namely with 100 μM nicotinamide and with 100 μM nicotinic acid (35, 36). However, neither of these NAD^+ precursors showed an effect on *E-cadherin*, *vimentin*, or *ZEB1* expression (Fig. 5*C*). Finally, MCF10A cells were transduced with a NAMPT isoform (NAMPT H247A) that has been reported previously to be cat-

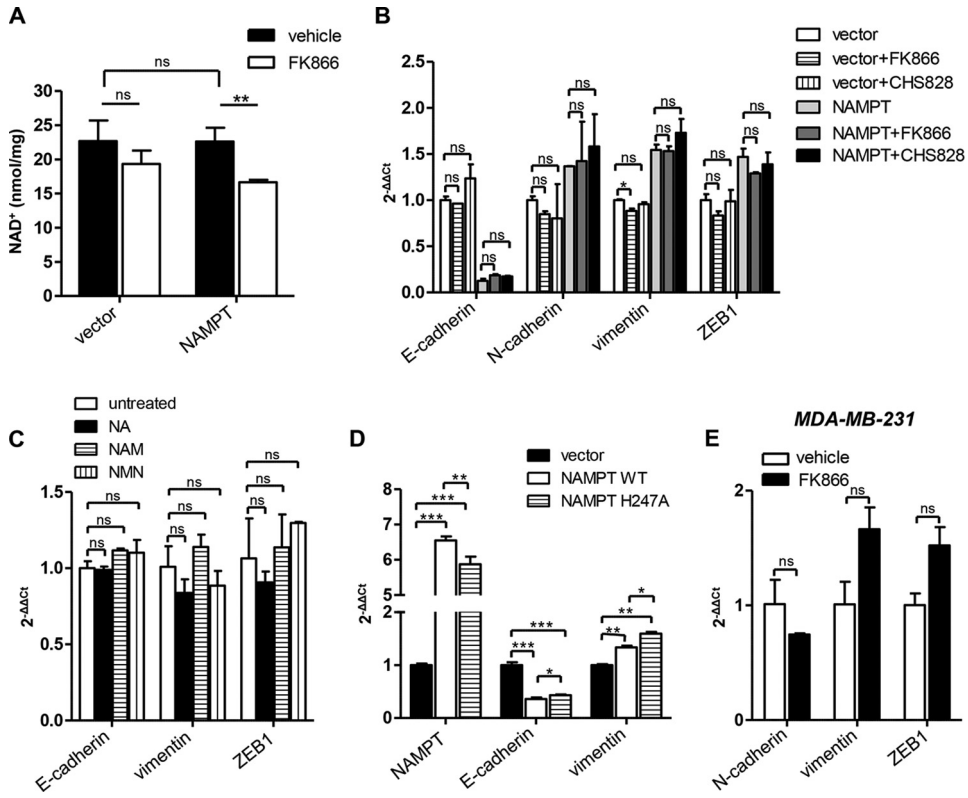

FIGURE 5. **NAMPT promotes EMT independent of its enzymatic activity.** *A*, 10^5 NAMPT-MCF10A or vector cells/well were incubated in 6-well plates for 48 h in the presence or absence of 300 nM FK866. Thereafter, cells were lysed in perchloric acid, and intracellular NAD^+ content was determined. *B*, NAMPT-MCF10A or vector cells were cultured in 6-well plates for 14 days in the presence or absence of 300 nM FK866 or CHS 828. Thereafter, cells were used for RNA extraction and *E-cadherin*, *N-cadherin*, *vimentin*, and *ZEB1* levels were quantified by QPCR. *C*, NAMPT-MCF10A or vector cells were cultured in 6-well plates for 14 days with or without 100 μM nicotinic acid (*NA*), nicotinamide (*NAM*), or nicotinamide mononucleotide (*NMN*). Thereafter, RNA was isolated, and *E-cadherin*, *vimentin*, and *ZEB1* mRNA levels were quantified by QPCR. *D*, 10^6 cells transduced with NAMPT, NAMPT H247A, or a control vector were plated in 10-cm Petri dishes. 48 h later, cells were used for RNA extraction, and *E-cadherin*, *vimentin*, and *NAMPT* mRNA levels were determined by QPCR. *E*, MDA-MB-231 cells were cultured in 6-well plates for 2 weeks in the presence or absence of 300 nM FK866. Thereafter, cells were used for RNA extraction, and *N-cadherin*, *vimentin*, and *ZEB1* levels were quantified by QPCR. *A*—*E*, *, $p < 0.05$; **, $p < 0.01$; ***, $p < 0.001$; *ns*, not statistically significant. One representative experiment of three is presented.

alytically inactive (37, 38). Both NAMPT-MCF10A and MCF10A cells expressing the catalytically inactive NAMPT exhibited a marked down-regulation in *E-cadherin* and *vimentin* up-regulation compared with control cells (Fig. 5*D*), although cells transduced with NAMPT H247A had slightly higher levels of *E-cadherin* compared with NAMPT-MCF10A cells. Taken together, these findings confirm that the loss of epithelial features and the expression of mesenchymal markers in NAMPT-MCF10A cells is independent of the enzymatic activity of this protein.

Experiments were also performed to determine whether FK866 would have any effect on the mesenchymal features of BC cells with an established EMT phenotype. To this end, MDA-MB-231 cells were selected because FK866 was found to minimally affect their growth (24, 20, and 27% growth inhibition at 72 h in response to 10 nM, 100 nM, and 1 μM FK866, respectively), while, at the same time, reducing intracellular NAD^+ by more than 50%. Conversely, BT549 and MDA-MD-468 were more sensitive to the growth-inhibiting effects of this drug (for BT549, 51, 54, and 67% growth inhibition at 72 h in response to 10 nM, 100 nM, and 1 μM FK866, respectively; for MDA-MD-468, 32, 38, and 41% growth inhibition at 72 h in response to 10 nM, 100 nM, and 1 μM FK866, respectively) and, therefore, were not selected for these experiments. In MDA-MB-231 cells, *E-cadherin* expression could not be monitored by QPCR because it was always below detectable levels. With respect to the expression of *N-cadherin*, *vimentin*, and *ZEB1*, no up- or down-regulation in response to FK866 could be documented (Fig. 5*F*). Therefore, consistent with the data obtained in MCF10A cells, in this mesenchymal BC cell line, NAMPT enzymatic activity did not seem to be involved in the maintenance of the mesenchymal features.

NAMPT Promotes EMT as an Extracellularly Released Soluble Factor—As mentioned previously, in addition to acting intracellularly, NAMPT protein is also secreted by cells through a non-canonical mechanism and is easily detected in cell culture media and in plasma (4, 39). eNAMPT acts as a cytokine with proinflammatory, prochemotactic, antiapoptotic, and proangiogenic effects (40–42). Notably, although eNAMPT has enzymatic activity, its effects as an extracellular protein were shown to be, at least in some instances, independent of it (4, 26, 37, 39). Therefore, we decided to assess a potential role of eNAMPT in the EMT phenotype of NAMPT-MCF10A cells. We were able to detect a strong increase in eNAMPT levels in cell supernatants from NAMPT-MCF10A cells. Although control MCF10A cells typically exhibited eNAMPT concentrations of less than 2 ng/ml in their supernatants, eNAMPT levels in the supernatants from NAMPT-MCF10A cells were similar to those detected with MDA-MB-231 and BT549 mesenchymal-like BC cells (typically ranging

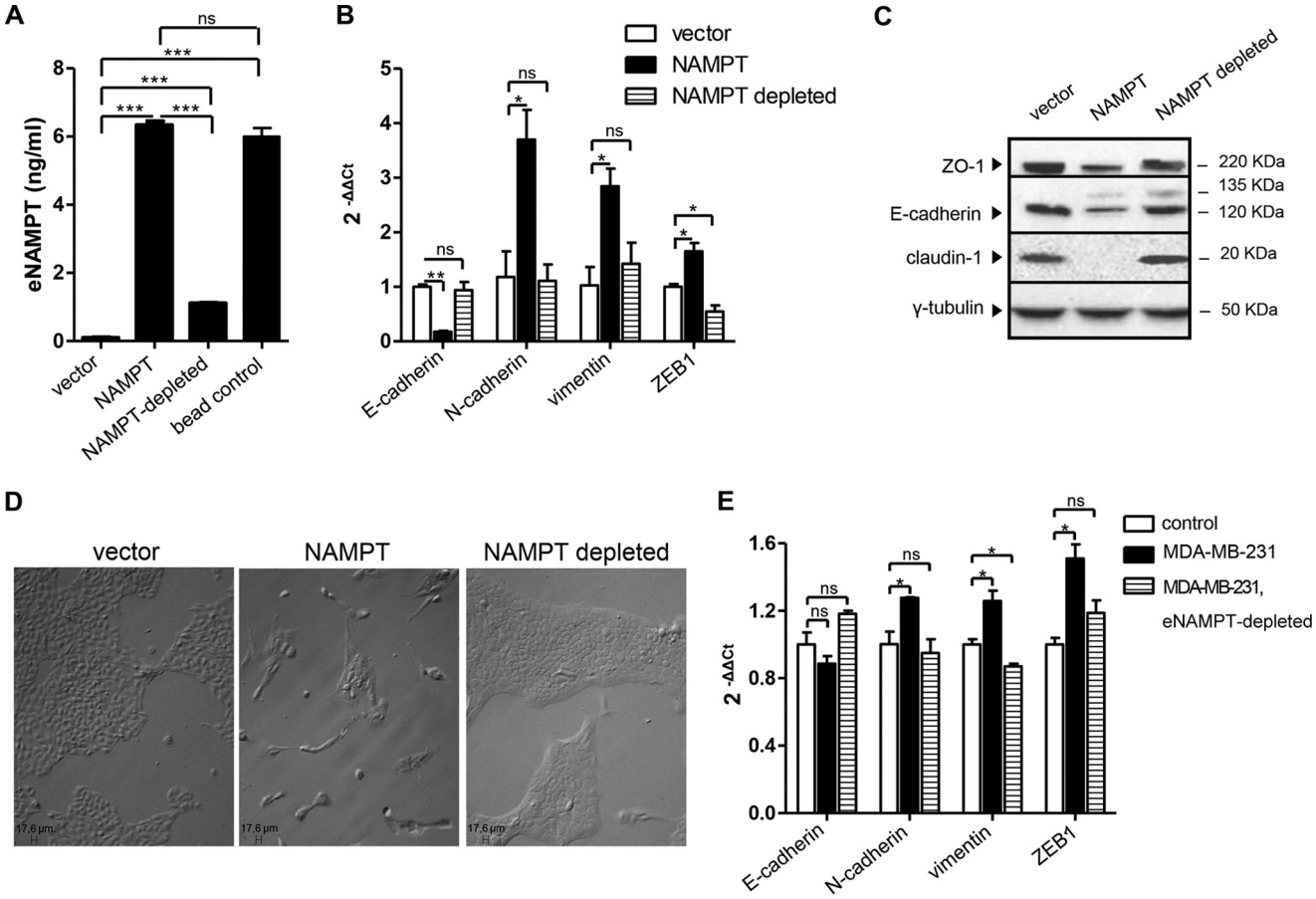

FIGURE 6. **NAMPT promotes EMT in MCF10A cells as an extracellularly released protein.** *A*, conditioned media were generated from NAMPT-MCF10A cells or vector cells (*vector*). The conditioned medium from NAMPT-MCF10A cells was incubated or not incubated (NAMPT) with magnetic beads that were coated (*NAMPT-depleted*) or not (*bead control*) with an anti-NAMPT antibody. Thereafter, the magnetic beads were removed, and eNAMPT levels in the cell media were determined by ELISA. *B* and *C*, MCF10A cells were incubated for 14 days in 6-well plates with conditioned medium from vector cells (*vector*), conditioned medium from NAMPT-MCF10A cells (*NAMPT*), or conditioned medium from NAMPT-MCF10A cells from which eNAMPT had been immunodepleted. Thereafter, cells were used for RNA extraction or for protein lysate generation. *E-cadherin*, *N-cadherin*, *vimentin*, and *ZEB1* mRNA levels were quantified by QPCR. ZO-1, E-cadherin, claudin, and γ-tubulin levels were detected by immunoblotting. *D*, MCF10A cells treated with conditioned media for 2 weeks as in *B* and *C* were imaged by light microscopy. *E*, plain MCF10A cells were cultured in 6-well plates with conditioned medium from MCF10A cells or from MDA-MB-231 cells (eNAMPT-immunodepleted or not). After 2 weeks, cells were used for RNA extraction, and *E-cadherin*, *N-cadherin*, *vimentin*, and *ZEB1* mRNA levels were quantified by QPCR. *A*, *B*, and *E*, *, $p < 0.05$; **, $p < 0.01$; ***, $p < 0.001$; *ns*, not statistically significant. One representative experiment of three is presented.

between 4–10 ng/ml). The increased levels of eNAMPT in NAMPT-MCF10A cells did not reflect passive leakage from dying cells because NAMPT-MCF10A and control cells both exhibited less than 10% spontaneous apoptosis (as detected by annexin V/propidium iodide staining and flow cytometry). In addition, Glc-6-PD activity in cell supernatants (taken as a marker for passive protein leakage from damaged cells), did not differ between the two cell types (data not shown). Conditioned medium from NAMPT-MCF10A or control cells was prepared and used to culture plain MCF10A cells for 14 days. Cells cultured in the presence of conditioned medium from NAMPT-MCF10A readily acquired a fibroblast-like morphology that was accompanied by a striking reduction in *E-cadherin* expression and by a consistent up-regulation of *N-cadherin*, *vimentin*, and *ZEB1* (see below). Therefore, these data indicated that the ability of overexpressed NAMPT to induce EMT was transmissible through the cell supernatants. To assess whether the presence of eNAMPT in the conditioned medium from NAMPT-MCF10A was required for EMT induction by the medium itself, we optimized an immunodepletion protocol that effectively reduced eNAMPT concentration (Fig. 6*A*). eNAMPT depletion completely abrogated the ability of the conditioned medium from NAMPT-MCF10A to induce EMT in MCF10A cells, as detected by monitoring *E-cadherin*, *N-cadherin*, and *vimentin* expression by QPCR (Fig. 6*B*) as well as ZO-1, E-cadherin, and claudin protein levels by immunoblotting (Fig. 6*C*). These findings were paralleled by the absence of a fibroblast-like morphology in the cells exposed to eNAMPT-depleted NAMPT-MCF10A supernatants (Fig. 6*D*). Interestingly, eNAMPT immunodepletion also prevented the up-regulation in *ZEB1* expression that was induced in MCF10A cells by NAMPT-MCF10A supernatants (Fig. 6*B*).

To determine whether an endogenous eNAMPT would also promote EMT in MCF10A cells, we utilized conditioned medium from MDA-MB-231 cells from which eNAMPT was either immunodepleted or not (MDA-MB-231 cells were found to grow normally in MCF10A medium, allowing us to prepare conditioned medium for MCF10A culture). In MDA-MB-231 medium, by utilizing the same method as above, a remarkable reduction from 6.2 to 0.2 ng/ml in eNAMPT concentration was

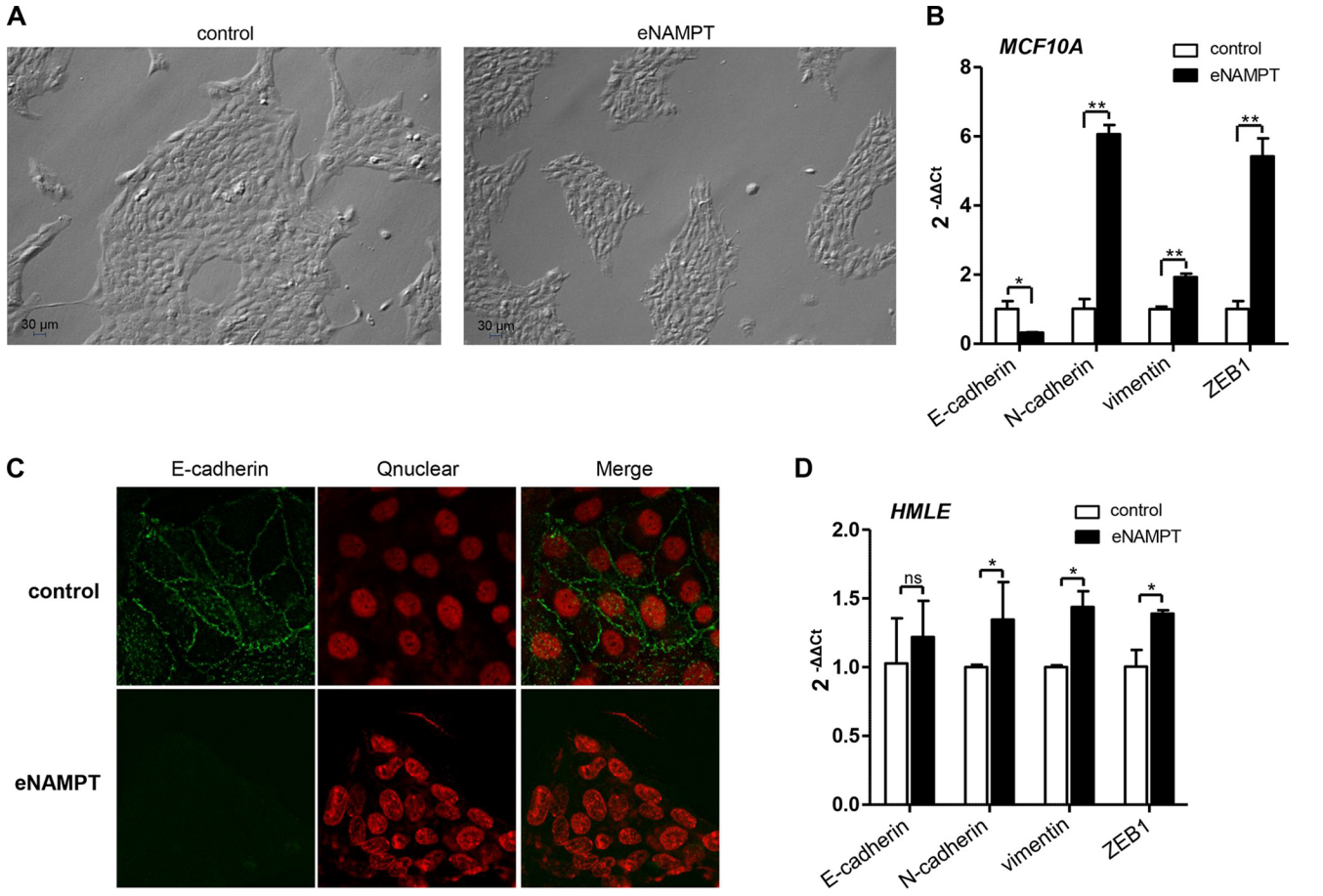

FIGURE 7. **Recombinant eNAMPT induces EMT in mammary epithelial cells.** *A* and *B*, MCF10A cells were incubated for 14 days with or without (control) 100 ng/ml recombinant human eNAMPT. Thereafter, cells were imaged by light microscopy (*A*) and, finally, used either for RNA extraction and *E-cadherin*, *N-cadherin*, *vimentin*, and *ZEB1* mRNA quantification by QPCR (*B*) or for confocal microscopy (*C*, E-cadherin detection, Qnuclear deep red (Qnuclear) nuclei staining, and their overlaps). *D*, HMLE cells were incubated for 14 days in 6-well plates with or without (*control*) 100 ng/ml recombinant human eNAMPT. Thereafter, RNA was extracted, and *E-cadherin*, *N-cadherin*, *vimentin*, and *ZEB1* mRNA levels were quantified by QPCR. *, $p < 0.05$; **, $p < 0.01$. *A–D*, one representative experiment of three is presented.

achieved. Conditioned medium from plain MCF10A cells or from MDA-MB-231 cells (with or without eNAMPT depletion) was utilized to culture plain MCF10A cells for 2 weeks. Despite the limits of this approach, it was of interest to observe that MDA-MB-231 medium induced *N-cadherin*, *vimentin*, and *ZEB1* up-regulation in MCF10A and that these effects were completely abrogated by eNAMPT depletion (Fig. 6*E*). Notably, despite the presence of high eNAMPT levels, MDA-MB-231 supernatants failed to induce *E-cadherin* down-regulation in MCF10A cells, which conceivably reflected the interference with eNAMPT-induced EMT by other factors secreted by MDA-MB-231 cells themselves.

Finally, as a confirmation of the ability of eNAMPT to induce EMT in mammary epithelial cells, we incubated plain MCF10A or HMLE cells with a commercially available recombinant human eNAMPT (generated in HEK 293 cells) for 2 weeks. In both cell lines, recombinant eNAMPT essentially recreated the effects of NAMPT overexpression (and of conditioned medium from NAMPT-overexpressing cells in the case of MCF10A cells). Namely, in MCF10A cells, recombinant eNAMPT induced the acquisition of an elongated, fibroblast-like morphology (Fig. 7*A*); *E-cadherin* down-regulation; as well as an increase in *N-cadherin, vimentin*, and *ZEB1* mRNA (Fig. 7*B*). E-cadherin down-regulation in response to eNAMPT was also readily documented by confocal microscopy (Fig. 7*C*). In HMLE cells, stimulation with eNAMPT led to *N-cadherin*, *vimentin*, and *ZEB1* up-regulation (Fig. 7*D*), but, again, in analogy to what was observed in response to NAMPT overexpression (Fig. 3*B*), *E-cadherin* down-regulation could not be detected in this cell line.

NAMPT Promotes EMT by Increasing TGFβ1 Production—Having established that NAMPT overexpression in mammary epithelial cells induces the expression of mesenchymal markers and of the transcription factor ZEB1, or even a full EMT, as in the case of MCF10A cells, that these effects are independent of NAMPT enzymatic activity, and that they are likely mediated by NAMPT in its secreted form (eNAMPT), it being sufficient to recreate them, we sought to determine the underlying mechanisms. To this end, we monitored the activation of EMT-promoting signaling cascades (25) in response to recombinant eNAMPT in MCF10A. Although no increase in phosphorylated ERK could be detected, both AKT and SMAD3 became phosphorylated in response to eNAMPT (Fig. 8*A*). To determine the role of the observed AKT activation in NAMPT-induced EMT, we treated MCF10A with 100 ng/ml eNAMPT for 2 weeks in the presence or absence of two validated AKT inhib-

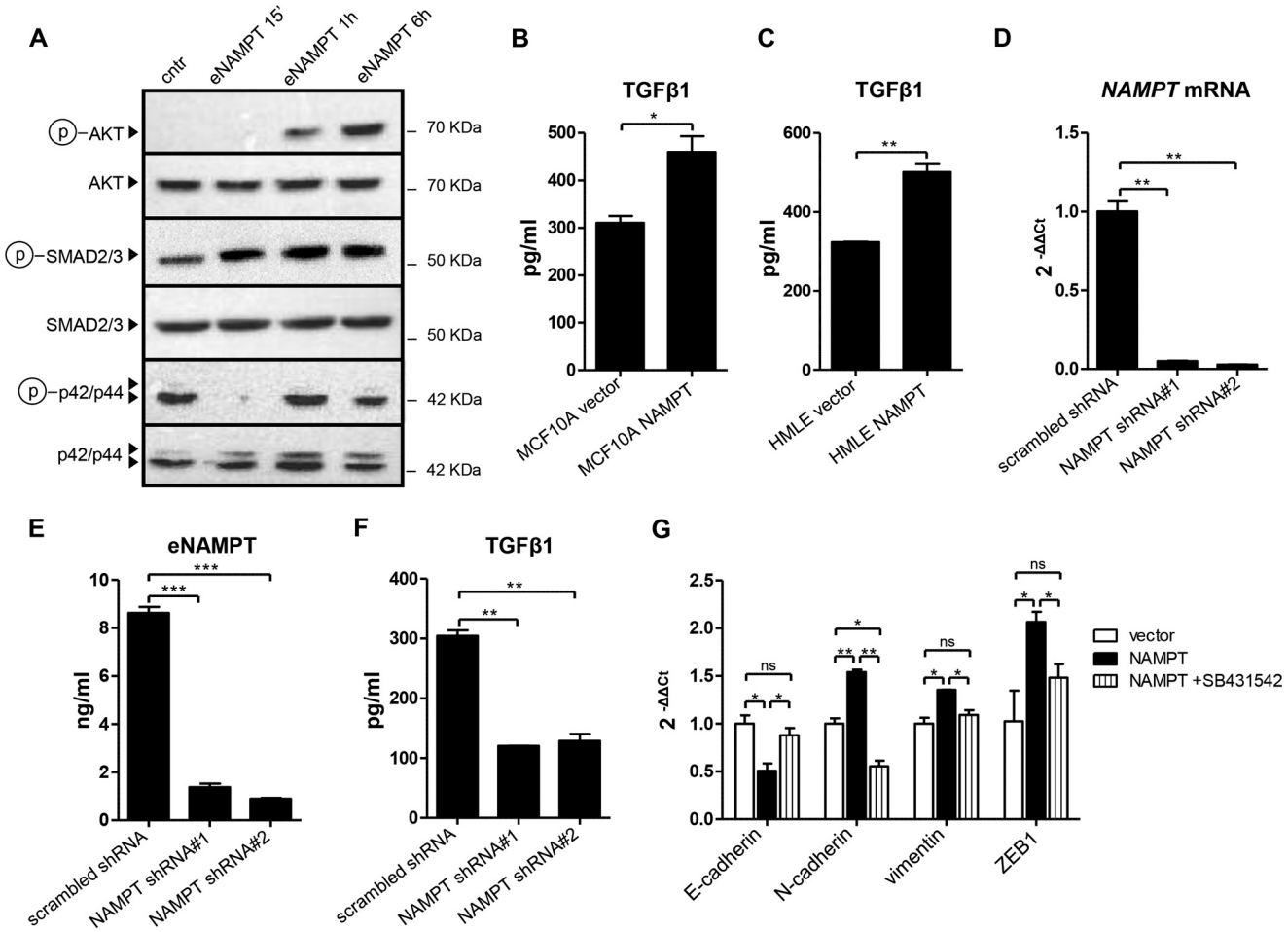

FIGURE 8. **NAMPT promotes TGFβ1 production, and EMT in NAMPT-overexpressing cells is mediated by TGFβ receptor signaling.** *A*, 2×10^5 MCF10A cells/well were plated in 6-well plates, allowed to adhere for 24 h, and subsequently stimulated for the indicated amounts of time with 100 ng/ml recombinant human eNAMPT. Thereafter, cells were lysed, and phospho-AKT (Ser-473), total AKT, phospho-ERK (p42/p44, Thr-202/Tyr-204), total ERK, phospho-SMAD3 (Ser-423/Ser-425), and total SMAD3 levels were detected by immunoblotting. *cntr*, control. *B* and *C*, 10^5 NAMPT-MCF10A, NAMPT-HMLE, or their respective vector control cells were plated in 2 ml of medium in each well of a 6-well plate. 48 h later, supernatants were harvested, and TGFβ1 levels were quantified by ELISA. *D–F*, MDA-MB-231 cells were lentivirally engineered to express a scrambled shRNA as a control or either one of two NAMPT-targeting shRNAs. Puromycin-selected cells were plated in equal numbers in 6-well plates (10^5 cells/well). 48 h later, cells were used for RNA extraction and QPCR quantification of *NAMPT* mRNA (*D*), or they were fixed with TCA and stained with SRB for subsequent normalization of the ELISA results. Cell supernatants were assayed for eNAMPT and TGFβ1 levels using commercially available ELISAs (E and *F*). *G*, NAMPT-MCF10A or their vector control cells were cultured for 2 weeks in 6-well plates. NAMPT-MCF10A cells were cultured in the presence of either 10 μM SB431542 or of vehicle (dimethyl sulfoxide). Subsequently, RNA was extracted, and *E-cadherin*, *N-cadherin*, *vimentin* and *ZEB1* mRNA levels were quantified by QPCR. *, $p < 0.05$; **, $p < 0.01$; *ns*, not statistically significant. *A–G*, one representative experiment of three is presented.

itors, AZD5363 and GDC-0068, or of the PI3K inhibitor LY294002. However, neither of the three compounds was able to revert the effects of eNAMPT (*E-cadherin* down-regulation and up-regulation of mesenchymal markers and of *ZEB1*) in this cell line (data not shown). Therefore, although possibly relevant for other biological effects, AKT activation did not mediate the EMT induced in MCF10A by eNAMPT.

SMAD3 belongs to the TGFβ signaling pathway, which is probably the most thoroughly characterized EMT-promoting signaling cascade (25). Because eNAMPT has been reported previously to induce the secretion of cytokines and growth factors (43), we reasoned that increased eNAMPT levels in cell supernatants from NAMPT-overexpressing cells could induce EMT by stimulating TGFβ1 production. In line with this hypothesis, both NAMPT-MCF10A and NAMPT-HMLE were found to have higher TGFβ1 levels in their supernatants compared with their respective control cells (Fig. 8, *B* and *C*). To evaluate whether NAMPT would also promote TGFβ1 production in a mesenchymal-like BC cell line, we silenced NAMPT in MDA-MB-231 cells utilizing two different shRNAs, both of which effectively reduced *NAMPT* mRNA as well as eNAMPT levels in cell supernatants (Fig. 8, *D* and *E*). Notably, opposite to what was observed by Santidrian *et al.* (3), in our hands, NAMPT silencing did reduce MDA-MB-231 proliferation, bringing the doubling time from 33.3 h for control cells (engineered with a scrambled shRNA) to 44.2 h and 43.9 h for cells in which NAMPT was silenced with NAMPT shRNA#1 or #2, respectively. That being so, as predicted, TGFβ1 concentration in supernatants from NAMPT-silent MDA-MB-231 cells was lower compared with the control cells (Fig. 8*F*). Finally, to assess which role the increased TGFβ1 production had in the EMT phenotype of NAMPT-MCF10A cells, we treated the latter with SB431542, a well characterized inhibitor of TGFβ receptor tyrosine kinase activity. SB431542 completely reverted *E-cadherin*

down-regulation as well as *vimentin*, *N-cadherin*, and *ZEB1* up-regulation in NAMPT-MCF10A cells, bringing the expression of these mRNAs to the levels found in control cells (Fig. 8*G*). Therefore, these findings indicate that the EMT observed in NAMPT-MCF10A cells was critically reliant upon TGFβ signaling.

DISCUSSION

In this work, we show that BC types with an aggressive clinical behavior, such as ER-negative, HER2-enriched, and basal-like BC, express high *NAMPT* levels. We demonstrate that NAMPT overexpression is sufficient to induce EMT in mammary epithelial cells. Importantly, the induction of these phenotypes by NAMPT is shown to be independent of its catalytic activity as an NAD^+ biosynthetic enzyme and to reflect its function as a cytokine (eNAMPT). Specifically, our data indicate the ability of NAMPT to increase the production of TGFβ1, which, in turn, is responsible for EMT induction. The translational relevance of these findings is highlighted by the fact that concentrations of eNAMPT that we found to induce EMT *in vitro* are commonly detected in patients (44–48), indicating that this protein is actually likely to contribute to EMT regulation and cancer in clinical contexts.

In MCF10A mammary epithelial cells, NAMPT overexpression (or stimulation with eNAMPT) induced a striking up-regulation of mesenchymal markers and of the transcription factor ZEB1. These changes were accompanied by *E-cadherin* down-regulation and by the acquisition of a $CD24^{low}/CD44^{high}$ phenotype, effects that are all consistent with the occurrence of a complete EMT (27). Interestingly, in NAMPT-HMLE cells (or in HMLE cells stimulated with eNAMPT), the increased expression of mesenchymal markers and ZEB1 was not paralleled by a reduction in E-cadherin. This discrepancy could be explained by the fact that, curiously, HMLE cells expressed NAMPT levels (both intracellular NAMPT and eNAMPT) that were significantly higher than those of MCF10A, essentially matching those observed in mesenchymal-like BC cell lines. Therefore, it is possible that high baseline NAMPT expression may make HMLE cells less sensitive to NAMPT overexpression and justify the incomplete EMT that these cells undergo. An alternative explanation for the persisting expression of E-cadherin in NAMPT-HMLE is offered by reports of cases of TGFβ1-induced EMT occurring without E-cadherin down-regulation. Maeda *et al.* (28) found that the E-cadherin expressed at the cell surface of NMuMG/E9 cells (another mammary epithelial cell line) did not change during TGFβ1-induced EMT. These authors proposed that, in their model, N-cadherin (which was up-regulated by TGFβ1) would act as a competitor of E-cadherin, suppressing its function and allowing EMT to occur. Therefore, because *N-cadherin* became readily up-regulated in NAMPT-HMLE cells, it is possible that a functional EMT actually occurred in these cells despite the persistence of E-cadherin.

The facts that mesenchymal-like BC cell lines express higher NAMPT levels compared with luminal cell lines, that a strong correlation exists in CCLE BC cell lines between the expression of *NAMPT* on the one hand and that of the mesenchymal markers *vimentin* and *fibronectin* and of the pro-EMT transcription factors *SNAI1/2* on the other hand, and that an association between *NAMPT* and *vimentin* expression is present in the METABRIC dataset, too, are all consistent with one another and with our *in vitro* data and strongly support the notion that NAMPT is an EMT-inducing protein.

The additional experiments we performed essentially converged to rule out that EMT induction in mammary epithelial cells overexpressing NAMPT is dependent on the enzymatic activity of this protein because no actual increase in intracellular NAD^+ levels was detected in NAMPT-MCF10A cells compared with vector cells; chemical NAMPT inhibitors did not revert the EMT even when applied early after cell transduction with NAMPT; cell supplementation with nicotinamide mononucleotide, the enzymatic product of NAMPT, did not induce EMT and neither did other NAD^+ precursors such as nicotinic acid or nicotinamide; and overexpression of a mutated, catalytically inactive NAMPT also resulted in a marked down-regulation of *E-cadherin* and in *vimentin* up-regulation in MCF10A cells. In addition, consistent with these data, treatment with FK866 had not effect on the EMT phenotype of MDA-MB-231 cells. These results are in line with those of Li *et al.* (26), who reported that eNAMPT protects macrophages from endoplasmic reticulum stress-induced apoptosis independent of its catalytic activity by promoting IL6 secretion, and with those of Liu *et al.* (37), according to which eNAMPT enzymatic activity is not required for it to induce IL8 production in pulmonary epithelial cells. In analogy with these two studies, in our models, a key biological effect of NAMPT (EMT) was also found to rely on the ability of its secreted form to stimulate the secretion of another cytokine (TGFβ1), which, in turn, was responsible for activating intracellular signaling cascades and for producing functional changes (SMAD3 activation and consequent EMT).

Notably, in the experiments aimed at assessing whether NAMPT also promotes TGFβ1 production in MDA-MB-231 cells, two NAMPT-silent MDA-MB-231 cell lines were generated. In these cell lines, *E-cadherin* mRNA remained below detectable levels and, therefore, could not be used to monitor potential modulations of the mesenchymal features of the cells. However, *vimentin* mRNA levels could be assessed, and they were found not to be affected by reduced NAMPT (data not shown). Therefore, in this model of mesenchymal-like BC, reducing cell exposure to eNAMPT was not sufficient to revert the established EMT phenotype.

Our findings of an association between *NAMPT* expression and ER-negative tumors are consistent with those of Lee *et al.* (20), who used IHC to detect NAMPT in BC and found that high NAMPT expression correlated with ER negativity and progesterone receptor negativity. In addition, similar to this previous study, the IHC analyses we performed also detected a preferential expression of NAMPT in tumor cells rather than in tumor stroma or in tumor-infiltrating leukocytes. However, although Lee *et al.* (20) found that NAMPT expression also correlated with tumor size, no correlation between *NAMPT* mRNA and tumor size was detected in our data set. It is also noteworthy that, in the study by Lee *et al.* (20), high NAMPT expression was also associated with poor disease-free and overall survival.

Our data indicate that the eNAMPT secreted by tumor cells (particularly by those expressing high levels of this protein) is likely sufficient to promote EMT. However, it is conceivable that the eNAMPT produced at distant sites (*i.e.* by circulating leukocytes or by adipose tissue) could also favor EMT and, thereby, carcinogenesis and metastasis. Dalamaga *et al.* (46) reported that, among postmenopausal women, serum eNAMPT levels are higher in patients with BC compared with healthy subjects and with patients with benign breast lesions. In the same study, a strong correlation between serum eNAMPT and the absence of ER and progesterone receptor in BC was detected (46). In addition to BC, plasma eNAMPT was found to be elevated in hepatocellular, gastric, endometrial, and colorectal carcinomas as well as in astrocytomas, myeloma, and male oral squamous cell carcinoma (4). Finally, circulating eNAMPT levels are typically increased in patients with obesity and type 2 diabetes (49). Because both conditions are known risk factors for many common cancers (10, 11), including BC, it is appealing to speculate that high eNAMPT concentrations in the extracellular environment of obese or diabetic patients could account, at least in part, for their predisposition to cancer.

Taken together with the available data on this enzyme, our results portrait NAMPT as a double-faced protein. On one hand, through its ability to rescue nicotinamide and increase intracellular NAD^+ levels, NAMPT can activate enzymes with tumor-suppressive properties such as SIRT1, SIRT3, SIRT6, and mitochondrial complex I (3, 50, 51). Dietary supplementation with nicotinamide (the substrate of NAMPT) or nicotinamide mononucleotide (the product of NAMPT) is expected to boost these effects, with possible benefits in terms of cancer prevention and treatment (52). On the other hand, when secreted into the extracellular environment, NAMPT (eNAMPT) may exert unwanted effects with the potential to promote tumorigenesis. These include its activity as an anti-apoptotic, chemotactic, proinflammatory, and proangiogenic factor and, as shown here, the ability to induce TGFβ1 production and, thereby, to promote EMT, with at least some of these functions being independent of the enzymatic activity of eNAMPT (4, 26, 37, 40–42). In such a scenario, therapeutic effects for agents that selectively targeted eNAMPT, such as monoclonal antibodies, nanobodies, or aptamers, can easily be anticipated. By selectively neutralizing eNAMPT, such agents could potentially be used to prevent EMT (and therefore, possibly, reduce the risk of metastasis) in cancers with high NAMPT expression (whether eNAMPT neutralization is also going to be effective at reverting established EMT phenotypes remains unclear and needs to be demonstrated) or in conditions in which circulating eNAMPT levels are excessively high, possibly predisposing to cancer, such as in obesity or type 2 diabetes (49).

In conclusion, our data indicate that high NAMPT levels in mammary epithelial cells promote EMT through a mechanism that is independent of the enzymatic activity of NAMPT but reflects its function as a cytokine with the ability to promote TGFβ1 production. On the basis of these data, eNAMPT-targeting therapeutic approaches appear to have a rationale as a means for preventing EMT and the disorders in which it plays a key pathophysiological role, including metastasis.

Acknowledgments—We thank Dr. Geoffrey Pickering (Robarts Research Institute, University of Western Ontario, London, Ontario, Canada) for providing valuable reagents, Dr. Robert A. Weinberg (Whitehead Institute for Biomedical Research, Cambridge, MA) for providing the HMLE cells, Dr. Filippo Ansaldi and Dr. Giancarlo Icardi (Department of Health Sciences, University of Genoa, Genoa, Italy) for the use of the BSL2+ facility, and Dr. Federico Carbone (Division of Cardiology, Foundation for Medical Researches, Department of Medical Specialties, University of Geneva, Geneva, Switzerland) for the analysis of NAMPT expression in primary tumor specimens.

REFERENCES

1. Imai, S., and Guarente, L. (2014) NAD and sirtuins in aging and disease. *Trends Cell Biol.* **24,** 464–471
2. Guarente, L. (2011) Franklin H. Epstein lecture: sirtuins, aging, and medicine. *N. Engl. J. Med.* **364,** 2235–2244
3. Santidrian, A. F., Matsuno-Yagi, A., Ritland, M., Seo, B. B., LeBoeuf, S. E., Gay, L. J., Yagi, T., and Felding-Habermann, B. (2013) Mitochondrial complex I activity and NAD^+/NADH balance regulate breast cancer progression. *J. Clin. Invest.* **123,** 1068–1081
4. Shackelford, R. E., Mayhall, K., Maxwell, N. M., Kandil, E., and Coppola, D. (2013) Nicotinamide phosphoribosyltransferase in malignancy: a review. *Genes Cancer* **4,** 447–456
5. Menssen, A., Hydbring, P., Kapelle, K., Vervoorts, J., Diebold, J., Lüscher, B., Larsson, L. G., and Hermeking, H. (2012) The c-MYC oncoprotein, the NAMPT enzyme, the SIRT1-inhibitor DBC1, and the SIRT1 deacetylase form a positive feedback loop. *Proc. Natl. Acad. Sci. U.S.A.* **109,** E187–196
6. Leary, R. J., Lin, J. C., Cummins, J., Boca, S., Wood, L. D., Parsons, D. W., Jones, S., Sjöblom, T., Park, B. H., Parsons, R., Willis, J., Dawson, D., Willson, J. K., Nikolskaya, T., Nikolsky, Y., Kopelovich, L., Papadopoulos, N., Pennacchio, L. A., Wang, T. L., Markowitz, S. D., Parmigiani, G., Kinzler, K. W., Vogelstein, B., and Velculescu, V. E. (2008) Integrated analysis of homozygous deletions, focal amplifications, and sequence alterations in breast and colorectal cancers. *Proc. Natl. Acad. Sci. U.S.A.* **105,** 16224–16229
7. Roxanis, I. (2013) Occurrence and significance of epithelial-mesenchymal transition in breast cancer. *J. Clin. Pathol.* **66,** 517–521
8. Hanahan, D., and Weinberg, R. A. (2011) Hallmarks of cancer: the next generation. *Cell* **144,** 646–674
9. Biganzoli, L., Wildiers, H., Oakman, C., Marotti, L., Loibl, S., Kunkler, I., Reed, M., Ciatto, S., Voogd, A. C., Brain, E., Cutuli, B., Terret, C., Gosney, M., Aapro, M., and Audisio, R. (2012) Management of elderly patients with breast cancer: updated recommendations of the International Society of Geriatric Oncology (SIOG) and European Society of Breast Cancer Specialists (EUSOMA). *Lancet Oncol.* **13,** e148–160
10. van den Brandt, P. A., Spiegelman, D., Yaun, S. S., Adami, H. O., Beeson, L., Folsom, A. R., Fraser, G., Goldbohm, R. A., Graham, S., Kushi, L., Marshall, J. R., Miller, A. B., Rohan, T., Smith-Warner, S. A., Speizer, F. E., Willett, W. C., Wolk, A., and Hunter, D. J. (2000) Pooled analysis of prospective cohort studies on height, weight, and breast cancer risk. *Am. J. Epidemiol.* **152,** 514–527
11. Noto, H., Goto, A., Tsujimoto, T., Osame, K., and Noda, M. (2013) Latest insights into the risk of cancer in diabetes. *J. Diabetes Investig.* **4,** 225–232
12. DeSantis, C., Ma, J., Bryan, L., and Jemal, A. (2014) Breast cancer statistics, 2013. *CA-Cancer J. Clin.* **64,** 52–62
13. Ferlay, J., Parkin, D. M., and Steliarova-Foucher, E. (2010) Estimates of cancer incidence and mortality in Europe in 2008. *Eur. J. Cancer* **46,** 765–781
14. Curtis, C., Shah, S. P., Chin, S. F., Turashvili, G., Rueda, O. M., Dunning, M. J., Speed, D., Lynch, A. G., Samarajiwa, S., Yuan, Y., Gräf, S., Ha, G., Haffari, G., Bashashati, A., Russell, R., McKinney, S., METABRIC Group,

Langerød, A., Green, A., Provenzano, E., Wishart, G., Pinder, S., Watson, P., Markowetz, F., Murphy, L., Ellis, I., Purushotham, A., Børresen-Dale, A. L., Brenton, J. D., Tavaré, S., Caldas, C., and Aparicio, S. (2012) The genomic and transcriptomic architecture of 2,000 breast tumours reveals novel subgroups. *Nature* **486,** 346–352

15. Vichai, V., and Kirtikara, K. (2006) Sulforhodamine B colorimetric assay for cytotoxicity screening. *Nat. Protoc.* **1,** 1112–1116
16. van der Veer, E., Ho, C., O'Neil, C., Barbosa, N., Scott, R., Cregan, S. P., and Pickering, J. G. (2007) Extension of human cell lifespan by nicotinamide phosphoribosyltransferase. *J. Biol. Chem.* **282,** 10841–10845
17. Cea, M., Cagnetta, A., Fulciniti, M., Tai, Y. T., Hideshima, T., Chauhan, D., Roccaro, A., Sacco, A., Calimeri, T., Cottini, F., Jakubikova, J., Kong, S. Y., Patrone, F., Nencioni, A., Gobbi, M., Richardson, P., Munshi, N., and Anderson, K. C. (2012) Targeting NAD^+ salvage pathway induces autophagy in multiple myeloma cells via mTORC1 and extracellular signal-regulated kinase (ERK1/2) inhibition. *Blood* **120,** 3519–3529
18. Bruzzone, S., Fruscione, F., Morando, S., Ferrando, T., Poggi, A., Garuti, A., D'Urso, A., Selmo, M., Benvenuto, F., Cea, M., Zoppoli, G., Moran, E., Soncini, D., Ballestrero, A., Sordat, B., Patrone, F., Mostoslavsky, R., Uccelli, A., and Nencioni, A. (2009) Catastrophic NAD^+ depletion in activated T lymphocytes through NAMPT inhibition reduces demyelination and disability in EAE. *PLoS ONE*, e7897
19. Barretina, J., Caponigro, G., Stransky, N., Venkatesan, K., Margolin, A. A., Kim, S., Wilson, C. J., Lehár, J., Kryukov, G. V., Sonkin, D., Reddy, A., Liu, M., Murray, L., Berger, M. F., Monahan, J. E., Morais, P., Meltzer, J., Korejwa, A., Jané-Valbuena, J., Mapa, F. A., Thibault, J., Bric-Furlong, E., Raman, P., Shipway, A., Engels, I. H., Cheng, J., Yu, G. K., Yu, J., Aspesi, P., Jr., de Silva, M., Jagtap, K., Jones, M. D., Wang, L., Hatton, C., Palescandolo, E., Gupta, S., Mahan, S., Sougnez, C., Onofrio, R. C., Liefeld, T., MacConaill, L., Winckler, W., Reich, M., Li, N., Mesirov, J. P., Gabriel, S. B., Getz, G., Ardlie, K., Chan, V., Myer, V. E., Weber, B. L., Porter, J., Warmuth, M., Finan, P., Harris, J. L., Meyerson, M., Golub, T. R., Morrissey, M. P., Sellers, W. R., Schlegel, R., and Garraway, L. A. (2012) The Cancer Cell Line Encyclopedia enables predictive modelling of anticancer drug sensitivity. *Nature* **483,** 603–607
20. Lee, Y. C., Yang, Y. H., Su, J. H., Chang, H. L., Hou, M. F., and Yuan, S. S. (2011) High visfatin expression in breast cancer tissue is associated with poor survival. *Cancer Epidemiol. Biomark. Prev.* **20,** 1892–1901
21. Parker, J. S., Mullins, M., Cheang, M. C., Leung, S., Voduc, D., Vickery, T., Davies, S., Fauron, C., He, X., Hu, Z., Quackenbush, J. F., Stijleman, I. J., Palazzo, J., Marron, J. S., Nobel, A. B., Mardis, E., Nielsen, T. O., Ellis, M. J., Perou, C. M., and Bernard, P. S. (2009) Supervised risk predictor of breast cancer based on intrinsic subtypes. *J. Clin. Oncol.* **27,** 1160–1167
22. Prat, A., Parker, J. S., Karginova, O., Fan, C., Livasy, C., Herschkowitz, J. I., He, X., and Perou, C. M. (2010) Phenotypic and molecular characterization of the claudin-low intrinsic subtype of breast cancer. *Breast Cancer Res.* **12,** R68
23. Mantovani, A., Marchesi, F., Porta, C., Sica, A., and Allavena, P. (2007) Inflammation and cancer: breast cancer as a prototype. *Breast* **16,** S27–33
24. Grivennikov, S. I., Greten, F. R., and Karin, M. (2010) Immunity, inflammation, and cancer. *Cell* **140,** 883–899
25. Lamouille, S., Xu, J., and Derynck, R. (2014) Molecular mechanisms of epithelial-mesenchymal transition. *Nat. Rev. Mol. Cell Biol.* **15,** 178–196
26. Li, Y., Zhang, Y., Dorweiler, B., Cui, D., Wang, T., Woo, C. W., Brunkan, C. S., Wolberger, C., Imai, S., and Tabas, I. (2008) Extracellular NAMPT promotes macrophage survival via a nonenzymatic interleukin-6/STAT3 signaling mechanism. *J. Biol. Chem.* **283,** 34833–34843
27. Mani, S. A., Guo, W., Liao, M. J., Eaton, E. N., Ayyanan, A., Zhou, A. Y., Brooks, M., Reinhard, F., Zhang, C. C., Shipitsin, M., Campbell, L. L., Polyak, K., Brisken, C., Yang, J., and Weinberg, R. A. (2008) The epithelial-mesenchymal transition generates cells with properties of stem cells. *Cell* **133,** 704–715
28. Maeda, M., Johnson, K. R., and Wheelock, M. J. (2005) Cadherin switching: essential for behavioral but not morphological changes during an epithelium-to-mesenchyme transition. *J. Cell Sci.* **118,** 873–887
29. Lehmann, B. D., Bauer, J. A., Chen, X., Sanders, M. E., Chakravarthy, A. B., Shyr, Y., and Pietenpol, J. A. (2011) Identification of human triple-negative breast cancer subtypes and preclinical models for selection of targeted therapies. *J. Clin. Invest.* **121,** 2750–2767
30. Rongvaux, A., Shea, R. J., Mulks, M. H., Gigot, D., Urbain, J., Leo, O., and Andris, F. (2002) Pre-B-cell colony-enhancing factor, whose expression is up-regulated in activated lymphocytes, is a nicotinamide phosphoribosyltransferase, a cytosolic enzyme involved in NAD biosynthesis. *Eur. J. Immunol.* **32,** 3225–3234
31. Bogan, K. L., and Brenner, C. (2008) Nicotinic acid, nicotinamide, and nicotinamide riboside: a molecular evaluation of NAD^+ precursor vitamins in human nutrition. *Annu. Rev. Immunol.* **28,** 115–130
32. Hasmann, M., and Schemainda, I. (2003) FK866, a highly specific noncompetitive inhibitor of nicotinamide phosphoribosyltransferase, represents a novel mechanism for induction of tumor cell apoptosis. *Cancer Res.* **63,** 7436–7442
33. Olesen, U. H., Christensen, M. K., Björkling, F., Jäättelä, M., Jensen, P. B., Sehested, M., and Nielsen, S. J. (2008) Anticancer agent CHS-828 inhibits cellular synthesis of NAD. *Biochem. Biophys. Res. Commun.* **367,** 799–804
34. Cerna, D., Li, H., Flaherty, S., Takebe, N., Coleman, C. N., and Yoo, S. S. (2012) Inhibition of nicotinamide phosphoribosyltransferase (NAMPT) activity by small molecule GMX1778 regulates reactive oxygen species (ROS)-mediated cytotoxicity in a p53- and nicotinic acid phosphoribosyltransferase1 (NAPRT1)-dependent manner. *J. Biol. Chem.* **287,** 22408–22417
35. Magnone, M., Bauer, I., Poggi, A., Mannino, E., Sturla, L., Brini, M., Zocchi, E., De Flora, A., Nencioni, A., and Bruzzone, S. (2012) NAD^+ levels control Ca^{2+} store replenishment and mitogen-induced increase of cytosolic Ca^{2+} by cyclic ADP-ribose-dependent TRPM2 channel gating in human T lymphocytes. *J. Biol. Chem.* **287,** 21067–21081
36. Grozio, A., Sociali, G., Sturla, L., Caffa, I., Soncini, D., Salis, A., Raffaelli, N., De Flora, A., Nencioni, A., and Bruzzone, S. (2013) CD73 protein as a source of extracellular precursors for sustained NAD^+ biosynthesis in FK866-treated tumor cells. *J. Biol. Chem.* **288,** 25938–25949
37. Liu, P., Li, H., Cepeda, J., Xia, Y., Kempf, J. A., Ye, H., Zhang, L. Q., and Ye, S. Q. (2009) Regulation of inflammatory cytokine expression in pulmonary epithelial cells by pre-B-cell colony-enhancing factor via a nonenzymatic and AP-1-dependent mechanism. *J. Biol. Chem.* **284,** 27344–27351
38. Wang, T., Zhang, X., Bheda, P., Revollo, J. R., Imai, S., and Wolberger, C. (2006) Structure of NAMPT/PBEF/visfatin, a mammalian NAD^+ biosynthetic enzyme. *Nat. Struct. Mol. Biol.* **13,** 661–662
39. Revollo, J. R., Körner, A., Mills, K. F., Satoh, A., Wang, T., Garten, A., Dasgupta, B., Sasaki, Y., Wolberger, C., Townsend, R. R., Milbrandt, J., Kiess, W., and Imai, S. (2007) NAMPT/PBEF/Visfatin regulates insulin secretion in β cells as a systemic NAD biosynthetic enzyme. *Cell Metab.* **6,** 363–375
40. Adya, R., Tan, B. K., Punn, A., Chen, J., and Randeva, H. S. (2008) Visfatin induces human endothelial VEGF and MMP-2/9 production via MAPK and PI3K/Akt signalling pathways: novel insights into visfatin-induced angiogenesis. *Cardiovasc. Res.* **78,** 356–365
41. Jia, S. H., Li, Y., Parodo, J., Kapus, A., Fan, L., Rotstein, O. D., and Marshall, J. C. (2004) Pre-B cell colony-enhancing factor inhibits neutrophil apoptosis in experimental inflammation and clinical sepsis. *J. Clin. Invest.* **113,** 1318–1327
42. Moschen, A. R., Kaser, A., Enrich, B., Mosheimer, B., Theurl, M., Niederegger, H., and Tilg, H. (2007) Visfatin, an adipocytokine with proinflammatory and immunomodulating properties. *J. Immunol.* **178,** 1748–1758
43. Montecucco, F., Cea, M., Cagnetta, A., Damonte, P., Nahimana, A., Ballestrero, A., Del Rio, A., Bruzzone, S., and Nencioni, A. (2013) Nicotinamide phosphoribosyltransferase as a target in inflammation-related disorders. *Curr. Top. Med. Chem.* **13,** 2930–2938
44. Tsouma, I., Kouskouni, E., Demeridou, S., Boutsikou, M., Hassiakos, D., Chasiakou, A., Hassiakou, S., and Baka, S. (2014) Correlation of visfatin levels and lipoprotein lipid profiles in women with polycystic ovary syndrome undergoing ovarian stimulation. *Gynecol. Endocrinol.* **30,** 516–519
45. de Luis, D. A., Aller, R., Gonzalez Sagrado, M., Conde, R., Izaola, O., and de la Fuente, B. (2013) Serum visfatin levels and metabolic syndrome criteria in obese female subjects. *Diabetes Metab. Res. Rev.* **29,** 576–581

46. Dalamaga, M., Archondakis, S., Sotiropoulos, G., Karmaniolas, K., Pelekanos, N., Papadavid, E., and Lekka, A. (2012) Could serum visfatin be a potential biomarker for postmenopausal breast cancer? *Maturitas* **71,** 301–308
47. Reddy, P. S., Umesh, S., Thota, B., Tandon, A., Pandey, P., Hegde, A. S., Balasubramaniam, A., Chandramouli, B. A., Santosh, V., Rao, M. R., Kondaiah, P., and Somasundaram, K. (2008) PBEF1/NAmPRTase/Visfatin: a potential malignant astrocytoma/glioblastoma serum marker with prognostic value. *Cancer Biol. Ther.* **7,** 663–668
48. Fazeli, M. S., Dashti, H., Akbarzadeh, S., Assadi, M., Aminian, A., Keramati, M. R., and Nabipour, I. (2013) Circulating levels of novel adipocytokines in patients with colorectal cancer. *Cytokine* **62,** 81–85
49. Chang, Y. H., Chang, D. M., Lin, K. C., Shin, S. J., and Lee, Y. J. (2011) Visfatin in overweight/obesity, type 2 diabetes mellitus, insulin resistance, metabolic syndrome and cardiovascular diseases: a meta-analysis and systemic review. *Diabetes Metab. Res. Rev.* **27,** 515–527
50. Bruzzone, S., Parenti, M. D., Grozio, A., Ballestrero, A., Bauer, I., Del Rio, A., and Nencioni, A. (2013) Rejuvenating sirtuins: the rise of a new family of cancer drug targets. *Curr. Pharm. Des.* **19,** 614–623
51. Santidrian, A. F., LeBoeuf, S. E., Wold, E. D., Ritland, M., Forsyth, J. S., and Felding, B. H. (2014) Nicotinamide phosphoribosyltransferase can affect metastatic activity and cell adhesive functions by regulating integrins in breast cancer. *DNA Repair* **S1568–7864,** 00222–00225
52. Imai, S. (2010) A possibility of nutriceuticals as an anti-aging intervention: activation of sirtuins by promoting mammalian NAD biosynthesis. *Pharmacol. Res.* **62,** 42–47